Title

Mechanistic Investigation of the Iron-Catalyzed Azidation of Alkyl C(sp 3)–H Bonds with Zhdankin's λ3-Azidoiodane

Journal

Journal of the American Chemical Society, 143(39)

ISSN

0002-7863

Authors

Day, Craig S
Fawcett, Alexander
Chatterjee, Ruchira
et al.

Publication Date

2021-10-06

DOI

10.1021/jacs.1c07330

Peer reviewed

HHS Public Access

Author manuscript

J Am Chem Soc. Author manuscript; available in PMC 2022 September 06.

Published in final edited form as:

J Am Chem Soc. 2021 October 06; 143(39): 16184–16196. doi:10.1021/jacs.1c07330.

Mechanistic Investigation of the Iron-Catalyzed Azidation of Alkyl C(sp^3)—H Bonds with Zhdankin's λ^3-Azidoiodane

Craig S. Day[†],
Department of Chemistry, University of California, Berkeley, California 94720, United States

Alexander Fawcett[†],
Department of Chemistry, University of California, Berkeley, California 94720, United States

Ruchira Chatterjee,
Molecular Biophysics and Integrated Bioimaging Division, Lawrence Berkeley National Laboratory, Berkeley, California 94720, United States

John F. Hartwig
Department of Chemistry, University of California, Berkeley, California 94720, United States

Abstract

An in-depth study of the mechanism of the azidation of C(sp^3)—H bonds with Zhdankin's λ^3-azidoiodane reagent catalyzed by iron(II)(pybox) complexes is reported. Previously, it was shown that tertiary and benzylic C(sp^3)—H bonds of a range of complex molecules underwent highly site-selective azidation by reaction with a λ^3-azidoiodane reagent and an iron(II)(pybox) catalyst under mild conditions. However, the mechanism of this reaction was unclear. Here, a series of mechanistic experiments are presented that reveal critical features responsible for the high selectivity and broad scope of this reaction. These experiments demonstrate the ability of the λ^3-azidoiodane reagent to undergo I—N bond homolysis under mild conditions to form λ-iodanyl and azidyl radicals that undergo highly site-selective and rate-limiting abstraction of a hydrogen atom from the substrate. The resultant alkyl radical then combines rapidly with a resting state iron(III)-azide complex, which is generated by the reaction of the λ^3-azidoiodane with the iron(II)(pybox) complex, to form the C(sp^3)—N_3 bond. This mechanism is supported by the independent synthesis of well-defined iron complexes characterized by cyclic voltammetry, X-ray diffraction, and EPR spectroscopy, and by the reaction of the iron complexes with alkanes and the λ^3-azidoiodane. Reaction monitoring and kinetic studies further reveal an unusual effect of the

Corresponding Author John F. Hartwig – Department of Chemistry, University of California, Berkeley, California 94720, United States; jhartwig@berkeley.edu.
[†]C.S.D. and A.F. contributed equally to this work.

Supporting Information
The Supporting Information is available free of charge at https://pubs.acs.org/doi/10.1021/jacs.1c07330.
Detailed experimental procedures and characterization data for all compounds (PDF)

Accession Codes
CCDC 2093525 contains the supplementary crystallographic data for this paper. These data can be obtained free of charge via www.ccdc.cam.ac.uk/data_request/cif, or by emailing data_request@ccdc.cam.ac.uk, or by contacting The Cambridge Crystallographic Data Centre, 12 Union Road, Cambridge CB2 1EZ, UK; fax: +44 1223 336033.

The authors declare no competing financial interest.

catalyst on the rate of formation of product and consumption of reactants and suggest a blueprint for the development of new processes leading to late-stage functionalization of C(sp^3)—H bonds.

Graphical Abstract

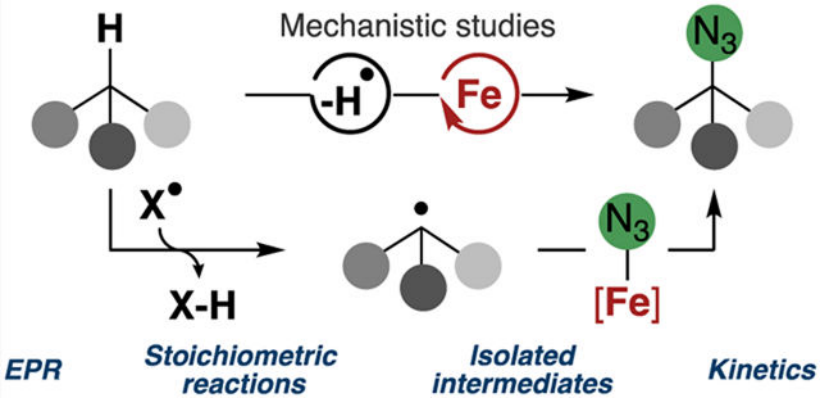

INTRODUCTION

Late-stage functionalization of C(sp^3)—H bonds within complex molecules has the potential to facilitate the synthesis of complex target molecules or to create chemical libraries by diversifying structures at specific positions.[1,2] Methods for the regioselective functionalization of C(sp^3)—H bonds in complex molecules with high functional-group tolerance, however, are rare, and studies to understand the mechanisms of such reactions are even less common.[3-5]

Nature has developed a suite of enzymes possessing iron-containing active sites, which catalyze the highly site-selective oxidation of C(sp^3)—H bonds of complex molecules,[6] and much effort has been expended to understand the mechanisms of these processes.[7,8] In concert, researchers have sought to mimic this reactivity of iron-containing enzymes to develop synthetic methods with small-molecule catalysts reacting by related mechanisms involving metal-oxo intermediates.[9] These complexes include both metal-porphyrin complexes that mimic the reactivity of hemoproteins and metal-amine and amidate complexes inspired by the reactivity of non-heme iron enzymes (Figure 1).[10-17]

While the reactions occurring through metal-oxo intermediates have led to valuable advances, we have sought processes that functionalize C—H bonds to form carbon—heteroatom bonds with first-row metal catalysts reacting without the intermediacy of oxo intermediates. Many such reaction pathways are possible and are challenging to delineate. Yet, these alternative pathways may offer selectivity and reactivity diverging from that of iron-oxo species and provide complementary reactivity for late-stage functionalization.

As part of these efforts, our group discovered that the combination of an iron catalyst with Zhdankin's hypervalent iodine reagent **1**[18,19] led to the azidation of C(sp^3)—H bonds in a mild and selective manner that was suitable for the functionalization of complex molecules

(Figure 2).[20,21] This method contrasts metal-free C(sp^3)—H azidation reactions,[19,22-25] which often lack sufficient selectivity and functional group tolerance to be applied to molecules that are dense in functional groups. Such C(sp^3)—H bond azidation reactions are important because the newly formed C(sp^3)—N_3 bond can be transformed into a range of high-value C(sp^3)—N bond-containing functional groups, such as amines, amides, and triazoles, all of which are important moieties in medicinal chemistry, therefore enabling the introduction of valuable functional groups into complex molecules at a late stage and at previously unfunctionalized sites. In addition, a particularly attractive application of azides is for “click” cycloadditions with alkynes, a reaction that could enable the straightforward attachment of fluorescent tags or bioconjugation to biotin,[26,27] processes that could facilitate the investigation of the biological activity of natural products and their targets.

While these studies and those of other researchers have led to valuable methodologies[25,28] such as Mn-,[29,30] Cu-,[31,32] or asymmetric Fe-catalyzed[33,34] azidation reactions, studies that have revealed more precise information about the mechanisms of these reactions are more limited. Such studies are made challenging by the ability of iron to readily undergo both one- or two-electron reactions and the paramagnetism of many iron complexes.[35-37] Consistent with this challenge, we reported preliminary studies including a primary kinetic isotope effect, which supports a turnover-limiting C(sp^3)—H bond cleavage during catalysis, but the identity of the critical species responsible for the site-selective cleavage of the C(sp^3)—H bond and for forming the C(sp^3)—N_3 bond was not revealed (Figure 3).

Herein, a detailed study of the iron-catalyzed C(sp^3)—H azidation reaction with hypervalent iodine reagent **1** is reported. This study clarifies the reaction components that undergo the crucial C—H bond-cleaving and C—N bond-forming steps and reveals the origin of the high site-selectivity and functional-group tolerance of this reaction. These studies provide evidence for the formation of carbon-centered radicals that are generated from hydrogen atom abstraction (HAA) between azidyl or λ^2-iodanyl radicals and aliphatic C(sp^3)—H bonds and reaction of the iron(II) precatalyst **1** to form an iron(III)—N_3, which acts as an electrophilic azide source to trap the alkyl radical and serves as the persistent radical in the system.[38,39] The rapid reaction of the alkyl radical by the iron(III)—N_3 complex contributes to the broad scope of the reaction.

RESULTS AND DISCUSSION

1. Proposed Mechanisms.

We considered several plausible classes of mechanisms for the iron(II) catalyzed C(sp^3)—H bond azidation reaction, on the basis of our preliminary mechanistic data,[20,21] the previously reported reactivity of **1**,[18,24] and the expected reactivity of an iron(II) complex. In one class of mechanism, a radical chain would be initiated by single-electron transfer from the iron(II) complex to **1**.[40] This electron transfer would generate azidyl and/or the corresponding λ^2-iodanyl radical, which could abstract a hydrogen atom from a C(sp^3)—H bond in the substrate.[24,41] DFT studies indicate that the λ^2-iodanyl radical generated from **1** contains significant spin density on both iodine and oxygen and is best described as a hybrid of resonance structures with radicals at these positions (Figure 3, potential H• abstractors, **1**•).[41] The transition state for hydrogen-atom abstraction is calculated to include an interaction of

the hydrogen in the C—H bond with the oxygen atom distal from iodine.[42] This abstraction of an H-atom would generate an alkyl radical, which would be trapped by **1** to form the alkyl azide product and (re)form an λ^2-iodanyl species that abstracts a C(sp^3)—H bond. In this manifold, the iron(II) complex would be responsible for initiating a radical chain and filling the role of the benzoyl peroxide used by Zhdankin in a previously reported C(sp^3)—H bond azidation with **1** (Figure 4a).[19]

In a second class of mechanism, a closed iron(II)/(III) catalytic cycle involving similar radical intermediates would occur. In this case, the iron(II) complex and **1** would react to form an iron(III)-azide species and the λ^2-iodanyl radical from **1**, the latter of which would abstract an H-atom from the substrate to generate an alkyl radical. This alkyl radical would be trapped by the iron(III)-azide complex to form the alkyl azide product and reform the original iron(II) species (Figure 4b).

In a third class of mechanism, the combination of an iron catalyst and Zhdankin's λ^3-azidoiodane would lead to an intermediate that cleaves the C(sp^3)—H bond without the intermediacy of azidyl or λ^2-iodanyl radicals. In this case, the iron(II) complex and **1** would react to form an iron(III) species that would cleave the C—H bond of the substrate. Pathways involving hydrogen-atom abstraction or concerted cleavage of the C(sp^3)—H bond, for example by a concerted metalation deprotonation of an C(sp^3)—H bond by a carboxylate to form a discrete iron-alkyl intermediate, could be envisioned. The alkyl complex could react by dissociation of an alkyl radical or by direct interaction with an azide transfer source (Figure 4c). [43,44]

In a fourth manifold, the mechanism could occur by a pathway analogous to iron-catalyzed oxidation reactions through an iron-oxo species.[9,45] In this case, reaction of a C(sp^3)—H bond with an iron-nitride or iron-nitrene complex could occur. Subsequent transfer of azide from **1** or an iron-azide complex would form the C(sp^3)—N bond.[29,33,46]

Finally, a fifth mechanism could occur by a hybrid of the previous four. In one such hybrid, oxidation of iron(II) by **1** would form an electrophilic iron(III)-azide complex. Separately, thermally induced homolysis of **1** could independently generate radicals that would undergo C(sp^3)—H HAA from the substrate to form an alkyl radical. The resultant radical could then selectively recombine with an iron(III)-azide to forge the C(sp^3)—N bond. Concurrent proton transfers could simultaneously exchange groups on iron and on iodine.

The described potential mechanistic pathways predict distinct steps by which the iron(II) complex reacts. Thus, we sought to distinguish between these mechanisms and hybrids of them by the synthesis and reactivity of the Fe(II) and Fe(III) complexes. These studies constitute the foundation of the investigation and are described in the next section.

2. Identification of the Catalytically Active Iron Species and Investigation of the Reaction of These Complexes with Zhdankin's λ^3-Azidoiodane and C-(sp^3)—H Bonds.

To determine the iron complexes involved in the catalytic reaction, a series of well-defined iron(II) and iron(III) species were synthesized and characterized, and their chemical

reactivity relevant to the azidation of C(sp^3)—H bonds with λ^3-azidoiodane **1** and substrates with tertiary C(sp^3)—H bonds was studied.

Iron(II) complexes (**L1**)$FeCl_2$ (**Fe-1**) and (**L1**)$Fe(OAc)_2$ (**Fe-2**) (**L1** = ^{i}PrPybox) were isolated and characterized. The reaction of a slight excess of $Fe(OAc)_2$ or $FeCl_2$ with 1 equiv of ^{i}PrPybox in acetonitrile or DCM generated blue solutions from which dark purple/blue solids were isolated (Figure 5a).[47] The (**L1**)$FeCl_2$ complex was crystallographically characterized as a trigonal bipyramidal complex.[48] The ATR-IR spectrum of (**L1**)$Fe(OAc)_2$ contained two acetate stretches with a >150 cm^{-1} difference between these asymmetric and symmetric frequencies, with the symmetric frequency shifted by 20 wavenumbers to higher frequency than those of $Fe(OAc)_2$,[49] indicating coordination of **L1** and κ^1-binding of the acetate; therefore, the structure of (**L1**)$Fe(OAc)_2$ is likely similar to the trigonal bipyramid of (**L1**)$FeCl_2$. Experiments on the reactions of **Fe-2** were performed first, followed by reactions of **Fe-1** (vide infra).

The kinetic competence of diacetate complex **Fe-2** was evaluated by conducting the azidation of isopentyl benzoate **2** with 10 mol% of **Fe-2** and **1**. This reaction resulted in a 77% yield of tertiary azide product **3**, which is comparable to that obtained from reactions with acetate complex **Fe-2** formed in situ (75% yield). Thus, complex **Fe-2** is competent to be a component of the pathway for azidation of tertiary C—H bonds.

The reaction of **Fe-2** with λ^3-azidoiodane **1** was investigated by allowing the two species to react in the absence of any substrate containing a reactive C(sp^3)—H bond and analyzing the organic and inorganic components by UV/vis absorbance, ^{1}H NMR, ATR-IR, and EPR spectroscopy, as well as MALDI-MS. Upon mixing equimolar quantities of **Fe-2** with λ^3-azidoiodane **1** in acetonitrile, an instantaneous color change from blue to a blood-red occurred. The UV/vis spectrum of the resulting reaction solution was characteristic of iron(III) species, with a strong absorbance band at λ_{max} = 480 nm.[50,51] The absence of the original absorbance band at λ_{max} = 587 nm showed that all of the starting **Fe-2** had reacted (Figure 5b).

The ^{1}H NMR spectrum of the reaction mixture also showed that diacetate **Fe-2** and **1** reacted. The paramagnetic signals of **Fe-2** disappeared, which was consistent with the full conversion of **Fe-2** indicated by UV/vis spectroscopy. In addition, quantification of the diamagnetic organic products revealed ca. 0.5 equiv of the initial 1.0 equiv of azidoiodane **1** was consumed. The expected organic products from homolytic cleavage of **1** and exclusive azide transfer to Fe(II), λ^3-iodane dimer **4** or 2-iodobenzoic acid **5**, did not form, suggesting that both azidyl and iodanyl units of **1** are transferred to Fe(II) to generate equimolar amounts of paramagnetic Fe(III)-azide and Fe(III)-carboxylate complexes.[52] Independent synthesis and isolation of the proposed products (**L1**)$Fe(OAc)_2N_3$ **Fe-3** and (**L1**)$Fe(OAc)_2$(2-I-benzoate) **Fe-4** were unsuccessful. However, ATR-IR spectroscopy of the reaction after removal of unreacted **1** and the solvent from the crude reaction mixture contained an absorbance at 2039 cm^{-1} (vs 2050 cm^{-1} of **1**),[19] which was characteristic of an iron-azide bond (Figure 5b),[50,51,53] and MALDI-MS analysis of the same solution revealed an ion corresponding to the iron-azide fragment $[(\mathbf{L1}\text{-}^i\text{Pr})Fe(OAc)(N_3)]^+$.[54] Furthermore, analysis of the reaction mixture by EPR spectroscopy revealed a mixture of high-spin Fe(III)

species, which partially fit $g = 4.39$ and $g = 2.02$. Therefore, one product of the reaction between λ^3-azidoiodane **1** and complex **Fe-2** was assigned as Fe(III)-azide **Fe-3** and the other as Fe(III)-benzoate **Fe-4**, based on the full consumption of the iron with just 0.5 equiv of azidoiodane **1**.[55]

Cyclic voltammetry of an iron(III) complex of **L1** and **1** revealed the redox properties of these reagents and their possible electron-transfer processes in the catalytic reaction. The cyclic voltammogram (CV) of **1** indicated an irreversible reduction E_{pc} at −0.43 V vs SCE, with no observable return oxidation peak E_{pa}, even at high scan rates.[56,57] The CV of iron(III) complex (**L1**)$FeCl_3$(**Fe-5**), which was prepared from the reaction of $FeCl_3$ with **L1**, contained a reversible reduction wave for $E^0(Fe^{III}/Fe^{II})$ at a more positive potential of −0.045 V vs SCE.[44] Because the reduction of **1** is irreversible, it was not possible to determine a formal reduction potential to compare with the reduction potential of (**L1**)$FeCl_3$. While the absolute difference in redox potentials is uncertain, the small difference between the formal potential of Fe(II/III) and irreversible reduction of **1** suggested that electron transfer from Fe(II) to **1** is possible (Figure 6).

To assess further if **Fe-5** could reduce **1**, we added 2 equiv of **1** to a solution of **Fe-5** and scanned across the negative potential. The resultant CV revealed a significantly higher current during the reduction of Fe(III) to Fe(II) (Figure 6, red trace) than during the reduction of **Fe-5** alone (Figure 6, blue trace); this greater current is consistent with repeating electrochemical reduction to Fe(II) due to chemical oxidation of Fe(II) to Fe(III) by **1**. In addition, the Fe(II)/Fe(III) oxidation peak was reversible in the absence of **1** but was irreversible in the presence of **1**, a result that is further consistent with the conversion of Fe(II) to Fe(III) by chemical oxidation of **1**.

To study iron complexes containing the $_i$PrPybox ligand that would be less dynamic than the acetates but catalytically relevant, we studied the analogous Fe-chloride complexes. The reaction of (**L1**)$FeCl_2$ (**Fe-1**) with λ^3-azidoiodane **1** was performed and analyzed by MALDI-MS, ^{1}H NMR, EPR, and UV/vis spectroscopy. The UV/vis spectra of this reaction displayed the same color change as observed previously with diacetate **Fe-2**, converting from blue to blood-red with a nearly identical spectrum containing an absorbance at λ_{max} = 494 nm. These data suggest the formation of complexes with analogous structures. Decay of paramagnetic ^{1}H NMR signals of **Fe-1** were also observed, along with the appearance of new, broadened paramagnetic ^{1}H NMR signals, consistent with oxidation of **Fe-1** to Fe(III). The MALDI mass spectrum contained fragments corresponding to the proposed iron(III)-azide and iron(III)-carboxylate species $[(\mathbf{L1}\text{-}^i\text{Pr})FeCl_2(N_3)]^+$ and $[(\mathbf{L1})FeCl_2(2\text{-I-benzoate})]^+$. EPR analysis was also consistent with high spin 5/2 complexes with rhombic distortions of the octahedral crystal field from features in the spectra at $g = 4.35$ and the second peak at $g = 2.03$ (Figure 7a).

While in-situ analysis provided data that were consistent with the generation of octahedral Fe(III) complex (**L1**)-$FeCl_2N_3$, an independent synthesis of this complex was performed to substantiate our assignment. Iron(III) azide complex (**L1**)$FeCl_2(N_3)$ (**Fe-6**) was isolated in quantitative yield as a dark-red solid after substitution of an azide for a chloride in (**L1**)$FeCl_3$(**Fe-5**) by treatment with an equimolar quantity of sodium azide (Figure 7b).

Spectroscopic characterization of **Fe-6** supported its assignment as (**L1**)$FeCl_2(N_3)$. The ATR-IR spectrum of **Fe-6** contained an absorbance at 2035 cm^{-1}, which is characteristic of an Fe-azide unit[50,51,53] and close to that observed for the species formed by the reaction of (**L1**)$Fe(OAc)_2$ and **1** (complex **Fe-3**, 2039 cm^{-1}, *vide supra*); the UV/vis spectrum contained an absorbance at λ_{max} = 479 nm, which was identical to that of the product of the reaction of (**L1**)$FeCl_2$ with **1** (Figure 7a).

The oxidation state, spin state, and geometry of azide **Fe-6** were assessed by EPR spectroscopy. The spectra (Figure 7a) contained one signal at g = 4.35 and a second signal at g = 2.03 were consistent with a high spin S = 5/2 complex with rhombic distortions of the octahedral crystal field. The paramagnetic ^{1}H NMR signals of **Fe-6** overlayed with signals observed in the ^{1}H NMR spectrum of the reaction between dichloride **Fe-1** and **1**, supporting the assertion that **Fe-6** forms from the reaction of **Fe-1** with **1**.[58]

The potential that the isolated iron(III)-azide complex **Fe-6**, or a close analog of this complex, is an intermediate in the catalytic azidation was assessed. Complex (**L1**)$FeCl_2(N_3)$ **Fe-6** catalyzed the azidation of isopentyl benzoate **2** to give 43% of the tertiary azide **3**, alongside 19% of the tertiary chloride product **3-Cl**, the latter of which presumably arose by the transfer of a chlorine atom from the Fe—Cl unit.[59]

The reactivity of isolated iron(III)-azide complex **Fe-6** with individual reaction components also was assessed. Heating iron(III)-azide complex **Fe-6** at 50 °C did not lead to reaction with isopentyl benzoate or with a fluorinated λ^3-azidoiodane (Figure 7c, the fluorine atom was present to monitor the reaction by ^{19}F NMR spectroscopy). In addition, (**L1**)Fe-$(OAc)_2$(2-I-benzoate) generated in situ did not isomerize *cis*-decalin to *trans*-decalin after heating at 50 °C for 24 h.[60] These results indicate that Fe(III) complexes, either isolated or generated in the catalytic process by the reaction of (**L1**)$Fe(OAc)_2$ with λ^3-azidoiodane **1**, are not involved in abstraction of the C(sp^3)—H bond.

Finally, to assess whether the iron(III)-azide complex **Fe-6** can transfer an azide moiety to an alkyl radical in the absence of an λ^3-azidoiodane, equimolar quantities of **Fe-6** and AIBN were heated in acetonitrile at 80 °C. This reaction gave α-cyano azide **9** in 50% yield (Figure 7c), indicating that the azide of **Fe-6** transfers to an alkyl radical.

The experimental results detailed here eliminate several possible mechanistic proposals of section 1. The Fe(II) complexes react rapidly with **1**, but we conclude, by tracking the fate of both organic and transition-metal species, that the reaction of **1** with the iron complex does not form free radicals involved in the catalytic process. Instead, iron(III)-azide and Fe(III)-carboxylate complexes form. These iron(III) species do not react with C(sp^3)—H bonds by a concerted metalation-deprotonation step, and heating azide **Fe-6** did not lead to reactions with C(sp^3)—H bonds. This lack of reactivity implies that the azide does not lead to other iron complexes, such as an iron(III)—nitride that could abstract a C—H bond. Instead, the iron(III)-azide reacts with an alkyl radical to transfer the azide and generate a C(sp^3)—N_3 bond. Therefore, the role of the iron catalyst in the C(sp^3)—H bond azidation reaction is likely to transfer the azide to an alkyl radical.

3. Understanding the Iron-Free Reactivity of 1.

The consumption of the azide and iodocarboxylate units of **1** by Fe(II) to form Fe(III) complexes and lack of reactivity of the Fe(III) complexes with C—H bonds led us to investigate the reactivity of **1** alone. Reactions of λ^3-azidoiodane **1** with C(sp^3)—H bonds to form alkyl azides have been reported by Zhdankin[19] at high temperatures in the presence of a radical initiator, and an uncatalyzed azidation of the tertiary C(sp^3)—H bond of *N*-phthaloyl leucine methyl ester with **1** was reported by Chen[61] to occur at 50 °C. These thermally initiated azidations of C(sp^3)—H bonds with **1** suggest that **1**, or derivatives of **1**, can abstract a C(sp^3)—H bond and transfer an azide group.[62]

Calculated bond dissociation energies of the N—I bond in **1** range from 27.8—35.4 kcal/mol.[24,63,64] If the true value lies at the lower end of this range, the homolysis of the N—I bond could occur under mild thermal conditions to generate azidyl radical and the corresponding λ^2-iodanyl radical, both of which have been demonstrated previously to abstract hydrogen atoms from C(sp^3)—H bonds.[24,64,65] Therefore, we hypothesized that λ^3-azidoiodane **1** generates the species that undergoes HAA in these azidations of C(sp^3)—H bonds.

To assess the ability of λ^3-azidoiodane **1** to undergo homolysis of the I—N bond to generate an azidyl radical and the λ^2-iodanyl radical, the reaction of **1** with *E*- and *Z*-stilbene was investigated (Figure 8). Under the standard conditions for the iron-catalyzed azidation of C(sp^3)—H bonds at 50 °C, but with replacement of the alkane with *E*- or *Z*-stilbene **10**, diazidation of the olefin occurred to give diazide **11** in 59—64% yield, depending on the starting isomer.[66] Under the same set of conditions, but with added TEMPO, the oxyazidation product **12** was formed in quantitative yield as a mixture of two diastereomers by the addition of an azidyl group and TEMPO across the C=C bond. (Figure 8). Without the iron(II) catalyst or TEMPO, however, no benzylic azide product was detected; instead, *Z*-stilbene simply isomerized to *E*-stilbene. In the absence of iron, but the presence of TEMPO, the oxyazidation product **12** again formed.

These reaction outcomes agree with the proposal that homolysis of the I—N bond of **1** occurs at 50 °C. Many publications have shown that stilbene reacts with azidyl radicals, even in the presence of iron(II) catalysts,[20,67-69] to form a benzylic radical. In the presence of the iron(III) complex, this benzylic radical forms diazide **11**; in the absence of iron, this intermediate reverts to *E*-stilbene, and in the presence of TEMPO this benzylic intermediate is trapped by TEMPO to form oxyazidation product **12**.

These observations suggest that the diazidation with iron occurs because an azide transfer reagent, most likely the Fe(III)-azide species described in section 2, reacts faster with the benzylic radical intermediate to form the diazide product than the benzylic radical reverts to stilbene. In the absence of iron, the azidation of the benzylic radical must occur by **1**, instead of the iron-azide complex, and the lack of azide product in the absence of iron indicates that transfer of the azide from **1** is slower than transfer by an iron azide and slower than reversion of the benzylic intermediate to stilbene.

The homolysis of the N—I bond of azidoiodane **1** was further investigated by heating **1** in acetonitrile and DMSO at 50 °C in the absence of an iron complex or substrate with a tertiary C(sp^3)—H bond (Figure 8b). The solubility of azidoiodane **1** in DMSO is greater than 267 mM, which is more than an order of magnitude higher than the solubility of **1** in MeCN (20.0 mM at 25 °C). Heating a solution of **1** in DMSO for 24 h consumed about half of **1** to form 23% of acid **5** and 16% of dimer **4**, whereas heating a suspension of **1** in acetonitrile at 50 °C for 24 h led to just 5% of 2-iodobenzoic acid **5** and 1% of dimer **4**, with the remainder being unreacted **1**. The greater conversion in DMSO than in acetonitrile suggests that the insolubility of **1** in MeCN causes the rate of homolysis to be lower than that in DMSO. These results also imply that the homolysis of **1** is reversible because heating of λ^3-azidoiodane **1** with a substrate containing a tertiary C(sp^3)—H bond in acetonitrile solvent leads to significant consumption of **1** (ca. 80% conversion), but heating in the absence of these partners led to only partial conversion; if the homolysis were irreversible, a much greater consumption of **1** would occur.[70]

Together, this series of experiments implied that the weak I—N bond of **1** could undergo spontaneous homolysis at the 50 °C temperature of the azidation of C(sp^3)—H bonds to form iodinane and azidyl radicals.

4. Investigation of the Azidation of *trans*- and *cis*-Decalin.

To obtain more information about the species that reacts with the alkyl C(sp^3)—H bonds and the species that transfers the azido group, we conducted a systematic investigation of the azidation of *trans*-decalin **6a** and *cis*-decalin **6b** (Figure 9). The combination of iron-catalyzed and uncatalyzed azidations of the tertiary C(sp^3)—H bonds in decalin allowed us to compare the selectivity of uncatalyzed and iron-catalyzed azidation reactions.

Under the standard reaction conditions with the combination of $Fe(OAc)_2$ and **L1** as catalyst, *trans*-decalin **6a** and *cis*-decalin **6b** were converted to the corresponding tertiary azides **7a** and **7b** with an identical *trans:cis* ratio of the two isomeric azide products of ca. 4.5:1 (Figure 9a, entries 1 and 2). These results indicate that reactions of both isomers proceed through an identical intermediate (Figure 9a, **Int-6a** and **Int-6b**) regardless of the starting isomer of decalin. These reactions were completely inhibited by the addition of 1.0 equiv of BHT or TEMPO.[33,61] Under conditions of added TEMPO, where 93% of the starting material was recovered, and no azidation was observed. Each of these results is consistent with the formation of an alkyl free-radical in the azidation reaction.

The reactions of *trans*-decalin and of *cis*-decalin (**6a** and **6b**) with **1**, in the absence of an iron catalyst, both formed the tertiary azide products with an identical 2.2:1 ratio of **7a** to **7b** (Figure 9a, entries 4 and 5). In addition, the unreacted *cis*-decalin **6b** had undergone nearly full isomerization to *trans*-decalin **6a** at the end of the reaction. This isomerization of **6b** to **6a** lends further support to the intermediacy of alkyl radicals[64] **Int-6a** and **Int-6b**, which interconvert (Figure 9a), and further indicates that cleavage of the C(sp^3)—H bond is reversible in the iron-free azidation. The lack of isomerization of *cis*- to *trans*-decalin (**6b** to **6a**) in the iron-catalyzed reaction indicates that formation of the alkyl radical is irreversible

in the presence of an iron azide, presumably due to the more rapid trapping of alkyl radicals by the iron azide than by **1**.

The difference in d.r. for the iron-catalyzed and iron-free reactions (ca. 4.5:1 vs ca. 2.2:1) further suggests that a different species transfers the azide to form the C(sp^3)—N_3 bond in the iron-catalyzed and uncatalyzed reactions. In the azidation reactions without iron, λ^3-azodoiodane **1** would be the species that reacts with the tertiary radical derived from decalin to give the azide products.[19,61] In the iron-catalyzed reaction, the iron-azide complex is likely to be the major species that transfers the azide unit to the alkyl radical.[21,29,33]

To determine if an iron-azide complex transfers the azido unit to the alkyl radical throughout the reaction, the ratio of the isomeric azide products was monitored as a function of time. If the iron complex were participating in a closed catalytic cycle involving an iron(II) species and an iron(III)-azide, then the reaction would contain a constant amount of the iron(III)-azide and would form a constant ratio of the *trans* and *cis* azidodecalin products (Figure 9b). If the iron complex initiated a radical-chain reaction, however, then only one equivalent of product per equivalent of iron complex would form with the higher ratio of *trans* to *cis* azidodecalin, and subsequent equivalents of the azidodecalin would form with the lower ratio. The *trans*-to-*cis* ratio of the reaction would gradually approach the 2.2:1 ratio of azide products observed when the reaction is conducted without an iron catalyst.

Under the standard conditions, analysis of aliquots removed at regular time intervals from the azidation reaction of *cis*-decalin showed that the ratio of the *trans:cis* isomers was a constant value of ca. 4.5:1 from 1 to 24 h and afforded 85% of the azidodecalin products after 24 h. This result indicates that the species that transfers the azido group is regenerated during the reaction and supports a closed catalytic cycle occurring through a combination of an iron(II) species and an iron(III)-azide. Conducting the same experiment, but without the addition of an iron complex, revealed that a 2.2:1 ratio of isomeric azide products was observed at all time points from 4 to 24 h and afforded 59% of the azide product after 24 h.

The relative rates for reactions of the tertiary decalinyl radical with λ^3-azidoiodane **1** and with the iron(III)-azide were studied by conducting the azidation reaction in DMSO, a solvent in which **1** is fully soluble at the concentration of the reactions (see section 3). Conducting the azidation of *cis*-decalin in DMSO under catalytic conditions that are otherwise identical to those in acetonitrile resulted in azide products with a *trans:cis* ratio of 3.5:1 (Figure 9a, entry 3), a value that falls between that obtained in acetonitrile solvent for the reactions with and without the iron catalyst. As observed for the reaction in acetonitrile, the azidation of *cis*-decalin by **1** in DMSO in the absence of an iron catalyst gave the tertiary azide products in a 2.2:1 ratio (entry 6). These ratios of isomers suggest that the alkyl radical reacts with both λ^3-azidoiodane **1** and the iron-azide when **1** is present at high concentration.

Given that the initial concentration of **1** in DMSO is approximately 20 times greater than the concentration of the iron catalyst (13 mM), the relative rate of trapping of the alkyl radical by the putative iron-azide complex must be approximately 20 times greater than trapping by **1** at these concentrations to maintain this ratio of *trans* to *cis* azide products. Therefore,

under the standard conditions comprising acetonitrile solvent in which the concentration of **1** is ca. 10-fold lower, the relative rates of trapping of this radical by the iron-azide complex and by **1** should be approximately 200:1. These results suggest that the iron-azide complex is the dominant species that transfers the azide when the azidation reaction is conducted in acetonitrile with an iron catalyst.

In addition to increasing the rate of the individual step of the trapping of the alkyl radical, the iron complex increases the rate of the overall reaction. Monitoring the uncatalyzed and iron-catalyzed azidation of isopentyl 4-fluorobenzoate (**13**) to 3-azido-isopentyl 4-fluorobenzoate (**14**) showed that the reaction of **13** under the standard conditions with the iron catalyst is faster than the uncatalyzed reaction by ca. 7 times. More details on the kinetics of the reaction are provided in section 6.

This set of experiments revealed several critical features of the azidation reaction: the azidation proceeds by formation of an alkyl radical intermediate in the presence or absence of the iron catalyst; a closed catalytic cycle involving an iron(II) complex and an iron(III)-azide is followed, and the iron(III)-azide is likely the dominant species that transfers the azidyl group to the alkyl radical. Although the iron complex does not cleave the C(sp^3)—H bond, the rate of the reaction is increased by the iron complex.

5 Investigating Species Involved in Hydrogen-Atom Abstraction.

The data in section 3 showed that homolysis of the N—I bond of **1** at 50 °C generates azidyl and λ^2-iodanyl radicals, one or both of which could abstract a hydrogen atom from a C(sp^3)—H bond (Figure 8 and Figure 9). Both λ^2-odanyl and azidyl radicals have been proposed in prior literature to undergo site-selective abstraction of tertiary C(sp^3)—H bonds,[24,46,61,64] a site-selectivity that matches that observed in the azidation reaction; therefore, the identity of the radical species that abstracts the hydrogen atom from the C(sp^3)—H bond in the azidation reaction was investigated.

To determine the fate of the benzoic acid core of the λ^3-azidoiodane reagent in the catalytic C(sp^3)—H bond azidation, catalytic reactions with fluorinated λ^3-azidoiodane 8 were studied. The reaction of a model substrate' isopentyl 4-fluorobenzoate (**13**), with **8** catalyzed by $Fe(OAc)_2$ and **L1** was conducted, and after 24 h, the full reaction mixture was dissolved in DMSO-d_6 and analyzed by ^{19}F NMR spectroscopy (Figure 10). Of the 2 equiv (0.40 mmol) of fluorinated λ^3-azidoiodane **8**, 1.04 equiv (0.21 mmol) was converted to 2-iodo-4-fluorobenzoic acid (**15**), 0.23 equiv (0.09 mmol) converted to dimer **16**, and 0.34 equiv (0.07 mmol) of **8** remained. Several additional unidentified fluorinated compounds formed in small quantities. The tertiary azide product **14** formed in 63% yield, and 34% of **13** remained. The formation of 2-iodo-4-fluorobenzoic acid as the primary product derived from **8** in this experiment is consistent with the formation of the λ^2-iodanyl radical under the reaction conditions and HAA from the tertiary alkyl C(sp^3)—H bond of **13** by this radical to form 2-iodo-4-fluorobenzoic acid.

As noted above, 0.23 equiv (0.09 mmol) of iodane dimer **16** was generated from the catalytic process under the standard conditions, likely by the reaction between benzoic acid **15** and fluoro λ^3-azidoiodane reagent **8** or by dimerization of the λ^2-iodanyl radical. The

independent reaction of λ^3-azidoiodane **1** with 2-iodobenzoic acid in MeCN-d_3, therefore, was performed to validate this proposal. This reaction for 30 min at room temperature formed iodinane dimer **4** and HN_3 (identified by ^{1}H NMR and IR spectroscopy) each in ca. 20% yield, along with 70% of unreacted **1**. This result is consistent with the direct reaction of the benzoic acid 5 with λ^3-azidoiodanes **1** to form dimer **4** and also suggests that the reverse reaction can occur. Our previous results on the thermolysis of **1** (section 3) also suggest that radical dimerization can generate dimer **4**, indicating both are viable pathways.

To test if the iodinane dimers **4** and **16** formed in the catalytic reaction outcompete **1** as an oxidant for Fe(II) or serve as a source of λ^2-iodanyl radicals by thermal homolysis, a series of experiments were conducted. Having shown previously that the iron(II) acetate complex **Fe-2** reacts stoichiometrically with carboxyiodane dimer **4** (section 2), we sought to assess whether this reaction was faster or slower than the reaction of Fe(II) with λ^3-azidoiodane **1**.

The reactions of **Fe-2** with **1** and with 4 were monitored by UV/vis spectroscopy. The disappearance of the diagnostic absorption of **Fe-2** at λ_{max} = 587 nm by the addition of **1** to **Fe-2** occurred within seconds, while the reaction of **Fe-2** with **4** was slower and occurred in ca. 3 min. This result fits with the reduction potentials of the λ^3-azidoiodane **1** and the carboxyiodane **4** (Figure 11). The CV of 4 consists of an irreversible reduction wave at −0.65 V, which is 0.2 V more negative than the irreversible reduction (E_p) wave of **1** (−0.43 V). These potentials explain why **Fe-2** reacts faster with λ^3-azidoiodane **1** than carboxyiodane 4 and further indicates that **4** will not significantly compete with **1** as an oxidant for Fe(II) in the catalytic reaction.

We also tested whether **4** would undergo spontaneous homolysis to form benzoyloxy radicals under the conditions of the catalytic process. To do so, we heated **4** with *cis*-decalin at 85 °C in acetonitrile for 2 days. If the benzoyloxy radical formed, then it would abstract a C—H bond from the decalin and lead to isomerization. However, no conversion of *cis*-decalin to *trans*-decalin was observed. This result implies that dimer **4** does not spontaneously homolyze to generate the λ^2-iodanyl radicals and re-enter the catalytic cycle at the temperature of the standard catalytic process.

To ascertain whether the λ^2-iodanyl or azidyl radical formed by homolysis of the N—I bond of **1**, or both, underwent HAA, a set of electronically differentiated λ^3-azidoiodanes was synthesized, and the effect of such electronic differences on the site-selectivity of the C(sp^3)—H bond azidation reaction was determined (Figure 12). If the electronic properties of this reagent influence regioselectivity, then the λ^2-iodanyl radical is one of, or is exclusively, the species that undergoes HAA of the C(sp^3)—H bond; if the electronic properties do not influence regioselectivity, then the λ^2-iodanyl radical is unlikely to be the species that undergoes HAA, and the azidyl radical is likely the radical that undergoes HAA.

The HAA by an aroyloxy radical containing fluorine substituents on the arene backbone previously was shown to occur at methylene C(sp^3)—H bonds over methine C(sp^3)—H bonds.[65] Therefore, to probe if modifying the electronic influence of λ^3-azidoiodane affected site-selectivity, the azidation of biphenyl **17**, which features two electronically similar, but sterically differentiated, secondary and tertiary benzylic C(sp^3)—H bonds, was

conducted with the fluorinated λ^3-azidoiodane reagents **8**, **18**, and **19**[71] and quantified by ^{1}H NMR spectroscopy (ratios ±0.01). The reaction with the original, unsubstituted λ^3-azidoiodane **1** gave a 1.38:1 ratio of tertiary:secondary azide products **20** and **21**, while the reaction with **8** gave a 1.25:1 ratio, the reaction with **18** gave a 1.18:1 ratio, and the reaction with **19** gave a 1.03:1 ratio. The measurable differences between these values demonstrates the electronic properties of the arene backbone of λ^3-azidoiodane has an effect on site-selectivity and is consistent with HAA by the 2-iodobenzoic acid portion of the λ^3-azidoiodane in the form of the λ^2-iodanyl radical. While azidyl radicals have been shown to undergo HAA to form HN_3, we were unable to determine the extent by which azidyl radicals contribute to HAA in the standard reaction from these experiments. However, measuring the pressure change under the standard reaction conditions, we were able to determine that only ca. 3% (0.06 equiv) of the starting 2 equiv of **1** is liberated as N_2 gas after 24 h. Thus, a minority of the azidyl radicals generated from **1** decompose to nitrogen gas, and this result is consistent with azidyl radicals contributing to hydrogen-atom abstraction of a C—H bond in the overall process.

6. Kinetic Studies of the Catalytic Reaction.

To enable the information obtained in the previous sections on individual steps and potential intermediates of the C(sp^3)—H bond azidation reaction to be assembled into a complete reaction mechanism, the kinetics of the catalytic process were studied. The initial rates of the azidation of isopentyl benzoate (2 or 13) with λ^3-azidoiodane **1** and iron(II) catalysts bearing **L1** or strongly coordinating **L2** (**L2** = 2,6-di(1*H*-pyrazol-1-yl)-pyridine) were measured with a range of initial concentrations of reaction components.[54] The reaction catalyzed by $Fe(OAc)_2$ and **L2** under the standard catalytic conditions with isopentyl benzoate **2** formed 76% yield of azide **3** with an initial rate that is similar to that of the reaction catalyzed by $Fe(OAc)_2$ and **L1** (**L1** = 3.2×10^{-6} M/s vs **L2** = 1.9×10^{-6} M/s). We conducted some of our studies with **L2** to avoid potential complications due to azidation of the tertiary C(sp^3)—H bond of ligand **L1** and because the binding of this ligand is stronger than that of the more hindered ligand.

Figure 13a shows the results of these kinetic studies. In acetonitrile with $Fe(OAc)_2$ and **L2** as catalyst, a clear first-order dependence of the reaction rate on the concentration of the alkyl benzoate **13** (67 to 333 mM) was observed. In this solvent with $Fe(OAc)_2$ and **L1** as catalyst, a clear first-order dependence of the rate on the concentration of iodane **1** also was observed at concentrations (58 to 145 mM) of **1** in which the reagent is soluble. While the reaction in acetonitrile is faster in the presence of 5.0 mol% iron than in the absence of iron (Figure 9c), the order of the reaction in the concentration of (**L1**)$Fe(OAc)_2$ in acetonitrile between 5.0 mol% and 20 mol% (Figure 13a) was zero. In DMSO, a solvent in which **1** is completely soluble, the dependence of the reaction rate also was found to be first-order in the concentration of both fluorinated isopentyl benzoate **13** and iodane **1** and zero-order in iron.[72]

The first-order dependence on isopentyl benzoate is consistent with the previously published primary kinetic isotope effect, indicating that C(sp^3)—H cleavage is rate limiting.[21] The kinetic data also are consistent with the generation of radicals from **1**, HAA from isopentyl

benzoate by these radicals, and rapid trapping of the radicals by the iron-azide complex, causing the HAA step to be rate-limiting. The greater rate of reaction in the presence of iron than in the absence of iron, then, originates from a change in the reversibility of the HAA step from reversible in the absence of iron to irreversible in the presence of iron, as demonstrated in section 4.

7. Investigating Iron Speciation during Catalysis.

The speciation of the iron during the catalytic reaction was investigated by UV/vis, EPR, and ^{1}H NMR spectroscopy, as well as MALDI—MS, to assess whether an iron-azide accumulates during catalysis. The synthesis and full characterization of (**L1**)$FeCl_2N_3$ are described in section 2; the catalytic reaction was conducted with (**L1**)$FeCl_2$ (**Fe-1**) as a precatalyst and evaluated at 30 min. This time-point was selected to minimize exchange of the anionic ligands in complexes of type (**L1**)$FeClN_3$(OCOR) and (**L1**)$FeN_3(OCOR)_2$ (R = *o*-I-C_6H_4). The UV/vis and ^{1}H NMR spectra of the reaction mixture both contained diagnostic features identical to the spectra of (**L1**)$FeCl_2N_3$ (Figure 13b). Likewise, the resonances in the EPR spectra of the catalytic reaction corresponding to the major complex are consistent with spin $S = 5/2$ and rhombic distortions of the octahedral crystal field with the same rhombic character as observed for (**L1**)$FeCl_2(N_3)$ (section 2, Figure 7). Finally, a mass fragment corresponding to [(**L1**-^{i}Pr)$FeCl_2(N_3)$]$^+$ was observed by MALDI-MS. These data all support an iron(III)-azide complex as a major iron complex present during the catalytic process.

8. Effect of Rapid Trapping of the Alkyl Radical on Reaction Scope.

The effect of faster radical trapping on the reactions of six natural product derivatives is shown by the data in Figure 14. Under the standard conditions for azidation in acetonitrile with 10 mol% of the iron catalyst, the C(sp^3)—H bonds of pinane and of a derivative of caryophyllene that are α to a cyclobutyl group underwent azidation to give tertiary azides in 80% and 44% yield, respectively,[20,21] without opening of the adjacent cyclobutyl ring (Figure 14). However, the same reactions conducted in the absence of an iron catalyst, in either acetonitrile or DMSO, led to complete decomposition of the terpene reactants. In these reactions, the HAA step generates an α-cyclobutyl radical, which is known to undergo ring opening to give an alkene.[73-76] In the iron-catalyzed azidation, trapping of the α-cyclobutyl radical with an iron(III)-azide, apparently, outcompetes ring opening to form the alkyl azide product.

In addition to this difference in outcomes of the reactions of this specific structural type, azidation of additional substrates in high yield was enabled by the iron catalyst. For example, azidation of the betulinic acid derivative containing multiple tertiary C(sp^3)—H bonds occurs in good yield under the iron-catalyzed reaction, whereas just traces of the azide form in the absence of iron. Likewise, the azidation of a leucine derivative and of the musk indane celestolide occurred in higher yields in the presence of the iron catalyst than in the absence of the catalyst. Although a small selection of substrates, these cases illustrate the effect of the enhanced rate of trapping of the intermediate alkyl radical on the azidation of small molecules and on the azidation of compounds with complex structure and multiple functional groups.

9. Mechanistic Proposal.

The conclusions from the described experiments support the mechanism in Figure 15. In this mechanism an iron(III)-azide complex traps an alkyl radical generated by HAA from a tertiary C(sp^3)—H bond of the substrate by the azidyl or λ^3-iodanyl radical. At the beginning of the reaction, when λ^3-azidoiodane **1** is added to the reaction mixture containing the substrate and iron(II) complex **Fe-2**, the iron(II) precatalyst reacts readily with **1** to generate iron(III)-azide **Fe-3** and iron(III)-carboxylate **Fe-4** in equimolar quantities.[77] These complexes do not abstract a hydrogen atom from the tertiary C(sp^3)—H bond of the substrate; instead, λ^3-iodane **1** undergoes spontaneous, reversible homolysis at 50 °C, independently of the iron species, to generate the azidyl radical and the accompanying λ^2-iodanyl radical. Both the λ^2-iodanyl and azidyl radicals derived from **1** then undergo rate-limiting HAA from the weakest C(sp^3)—H bond of the alkane to form an alkyl radical.

The alkyl radical that is generated can react with either the iron(III)-azide, formed by the rapid reaction of Fe(II) with **1**, or with λ^3-azidoiodane **1** itself; however, the strong polarity match between the nucleophilic alkyl radical and electrophilic iron(III)-azide favors reaction with the iron(III)-azide by a ratio that is approximately 200:1 at the concentrations of the catalytic reaction (section 4). The reactivity of the alkyl radical with the iron azide is analogous to the selective cross-coupling observed between alkyl radicals and persistent radicals.[38,39]

By contrast, trapping of the alkyl radical (formed by the same reversible homolysis of **1** at 50 °C) with the λ^3-azidoiodane **1** in the uncatalyzed reaction is slower. This trapping is sufficiently slow that transfer of the hydrogen atom from the benzoic acid[42,78] or hydrazoic acid[64] or both to the alkyl radical to regenerate the C(sp^3)—H bond competes with the trapping of the alkyl radical to form the alkyl azide. Together, these experiments delineate critical aspects of the iron-catalyzed and uncatalyzed azidation reactions and describe the features responsible for causing the yield to be higher and the scope to be broader with the iron catalyst.

SUMMARY AND CONCLUSIONS

This study has probed deeply into the mechanism of the iron-catalyzed azidation of alkyl C(sp^3)—H bonds with Zhdankin's λ^3-azidoiodane reagent. Monitoring of the stoichiometric oxidation of Fe(II) by **1** showed the formation of iron(III)-azide complexes. Through independent synthesis, the fundamental reactivity of (**L1**)$FeCl_2(N_3)$ (**Fe-6**) was investigated and was demonstrated to include rapid reaction with alkyl radicals to form C(sp^3)—N_3 bonds, rather than to participate in HAA of C(sp^3)—H bonds. A comparison of the reactivity of **1** in uncatalyzed and iron-catalyzed reactions of stilbene and decalin showed that homolysis of **1** occurred under mild conditions to generate the λ^2-iodanyl and azidyl radicals. These radicals derived from **1** undergo HAA of C(sp^3)—H bonds to generate alkyl radicals that react rapidly with iron-azide complexes. Kinetic data indicate that HAA is the rate-limiting step during the catalytic transformation and that the iron azide reacts after HAA. Monitoring of the catalytic reaction showed the identity of the iron(III)-azide species

that is the resting state of the catalyst, and that an iron azide, which reacts rapidly with alkyl radicals to deliver the C(sp^3)—N_3 bonds, accumulates in the catalytic system.

The features of the mechanism of the reaction that create the ability to conduct late-stage azidations of complex molecules include the selective abstraction of a hydrogen atom from a tertiary C(sp^3)—H bond and rapid trapping of the alkyl radical intermediates by the iron azide. This rapid trapping outpaces deleterious side reactions, such as reverse HAA, rearrangement, and fragmentation of the alkyl radical.

This beneficial effect of the catalyst on the reaction outcome by affecting the rate of the steps that form product without affecting the steps that consume reactants is unusual. The rate of formation of the azidation product is higher in the presence of the iron catalyst, leading to large effects on reaction yield, but the rate of decay of reactant is zero order in catalyst above a certain range of catalyst loading, including the loading of catalyst in the standard reaction conditions. Taken together, the features of this reaction revealed here suggest a blueprint for the development of new processes capable of the late-stage functionalization of C(sp^3)—H bonds.

Supplementary Material

Refer to Web version on PubMed Central for supplementary material.

ACKNOWLEDGMENTS

We acknowledge Zachary Herrera, Dr. Ankit Sharma, and Dr. Rashad R. Karimov for conducting preliminary mechanistic investigations. This work was supported by the NIH (R35 GM130387), and we thank the College of Chemistry's NMR facility for resources provided and the staff for their assistance. Instruments in the CoC-NMR are supported in part by NIH S10OD024998. We thank Dr. Nicholas Settineri for X-ray crystallography (NIH S10-RR027172). The EPR work was supported by the Director, Office of Science, Office of Basic Energy Sciences (OBES), Division of Chemical Sciences, Geosciences, and Biosciences of the Department of Energy (DOE) (contract No. DE-AC02-05CH11231). C.S.D. thanks the European Union's Horizon 2020 under the Marie Curie PREBIST grant agreement 754558.

REFERENCES

(1). Hong B; Luo T; Lei X Late-Stage Diversification of Natural Products. ACS Cent. Sci 2020, 6 (5), 622–635. [PubMed: 32490181]

(2). Cernak T; Dykstra KD; Tyagarajan S; Vachal P; Krska SW The medicinal chemist's toolbox for late stage functionalization of drug-like molecules. Chem. Soc. Rev 2016, 45 (3), 546–576. [PubMed: 26507237]

(3). Yang Q; Wang Y-H; Qiao Y; Gau M; Carroll PJ; Walsh PJ; Schelter EJ Photocatalytic C—H activation and the subtle role of chlorine radical complexation in reactivity. Science 2021, 372 (6544), 847–852. [PubMed: 34016778]

(4). Chu JCK; Rovis T Complementary Strategies for Directed C(sp^3)—H Functionalization: A Comparison of Transition-Metal-Catalyzed Activation, Hydrogen Atom Transfer, and Carbene/Nitrene Transfer. Angew. Chem., Int. Ed 2018, 57 (1), 62–101.

(5). Crabtree RH; Lei A Introduction: CH Activation. Chem. Rev 2017, 117 (13), 8481–8482. [PubMed: 28697603]

(6). Denisov IG; Makris TM; Sligar SG; Schlichting I Structure and Chemistry of Cytochrome P450. Chem. Rev 2005, 105 (6), 2253–2278. [PubMed: 15941214]

(7). Meunier B; De Visser SP; Shaik S Mechanism of Oxidation Reactions Catalyzed by Cytochrome P450 Enzymes. Chem. Rev 2004, 104 (9), 3947–3980. [PubMed: 15352783]

(8). Guengerich FP Mechanisms of Cytochrome P450-Catalyzed Oxidations. ACS Catal. 2018, 8 (12), 10964–10976. [PubMed: 31105987]

(9). Baglia RA; Zaragoza JPT; Goldberg DP Biomimetic Reactivity of Oxygen-Derived Manganese and Iron Porphyrinoid Complexes. Chem. Rev 2017, 117 (21), 13320–13352. [PubMed: 28991451]

(10). White MC; Zhao J Aliphatic C—H Oxidations for Late-Stage Functionalization. J. Am. Chem. Soc 2018, 140 (43), 13988–14009. [PubMed: 30185033]

(11). Fawcett A Advances in the catalyst- and reagent-controlled site-divergent intermolecular functionalization of C(sp^3)-H bonds. Pure Appl. Chem 2020, 92 (12), 1987–2003.

(12). Gómez L; Garcia-Bosch I; Company A; Benet-Buchholz J; Polo A; Sala X; Ribas X; Costas M Stereospecific C—H Oxidation with H_2O_2 Catalyzed by a Chemically Robust Site-Isolated Iron Catalyst. Angew. Chem., Int. Ed 2009, 48 (31), 5720–5723.

(13). Chen MS; White MC A Predictably Selective Aliphatic C—H Oxidation Reaction for Complex Molecule Synthesis. Science 2007, 318 (5851), 783–787. [PubMed: 17975062]

(14). Costas M; Mehn MP; Jensen MP; Que L Dioxygen Activation at Mononuclear Nonheme Iron Active Sites: Enzymes, Models, and Intermediates. Chem. Rev 2004, 104 (2), 939–986. [PubMed: 14871146]

(15). Rohde J-U; In J-H; Lim MH; Brennessel WW; Bukowski MR; Stubna A; Munck E; Nam W; Que L Crystallographic and Spectroscopic Characterization of a Nonheme Fe(IV)═O Complex. Science 2003, 299 (5609), 1037–1039. [PubMed: 12586936]

(16). Milan M; Salamone M; Costas M; Bietti M The Quest for Selectivity in Hydrogen Atom Transfer Based Aliphatic C—H Bond Oxygenation. Acc. Chem. Res 2018, 51 (9), 1984–1995. [PubMed: 30080039]

(17). Collins TJ; Ryabov AD Targeting of High-Valent Iron-TAML Activators at Hydrocarbons and Beyond. Chem. Rev 2017, 117 (13), 9140–9162. [PubMed: 28488444]

(18). Zhdankin VV; Kuehl CJ; Krasutsky AP; Formaneck MS; Bolz JT Preparation and chemistry of stable azidoiodinanes: 1-Azido-3,3-bis(trifluoromethyl)-3-(1H)-1,2-benziodoxol and 1-Azido-1,2-benziodoxol-3-(1H)-one. Tetrahedron Lett. 1994, 35 (52), 9677–9680.

(19). Zhdankin VV; Krasutsky AP; Kuehl CJ; Simonsen AJ; Woodward JK; Mismash B; Bolz JT Preparation, X-ray Crystal Structure, and Chemistry of Stable Azidoiodinanes Derivatives of Benziodoxole. J. Am. Chem. Soc 1996, 118 (22), 5192–5197.

(20). Karimov RR; Sharma A; Hartwig JF Late Stage Azidation of Complex Molecules. ACS Cent. Sci 2016, 2 (10), 715–724. [PubMed: 27800554]

(21). Sharma A; Hartwig JF Metal-catalysed azidation of tertiary C—H bonds suitable for late-stage functionalization. Nature 2015, 517 (7536), 600–604. [PubMed: 25631448]

(22). Krasutsky AP; Kuehl CJ; Zhdankin VV Direct Azidation of Adamantane and Norbornane by Stable Azidoiodinanes. Synlett 1995, 1995 (10), 1081–1082.

(23). Magnus P; Lacour J New Trialkylsilyl Enol Ether Chemistry. Direct β-Azido Functionalization of Triisopropylsilyl Enol Ethers. J. Am. Chem. Soc 1992, 114 (2), 767–769.

(24). Huang X; Groves JT Taming Azide Radicals for Catalytic C—H Azidation. ACS Catal. 2016, 6 (2), 751–759.

(25). Sivaguru P; Ning Y; Bi X New Strategies for the Synthesis of Aliphatic Azides. Chem. Rev 2021, 121 (7), 4253–4307. [PubMed: 33635623]

(26). Fantoni NZ; El-Sagheer AH; Brown T A Hitchhiker's Guide to Click-Chemistry with Nucleic Acids. Chem. Rev 2021, 121 (12), 7122–7154. [PubMed: 33443411]

(27). Meldal M; Tornøe CW Cu-Catalyzed Azide-Alkyne Cycloaddition. Chem. Rev 2008, 108 (8), 2952–3015. [PubMed: 18698735]

(28). Goswami M; De Bruin B Metal-Catalysed Azidation of Organic Molecules. Eur. J. Org. Chem 2017, 2017 (8), 1152–1176.

(29). Meyer TH; Samanta RC; Del Vecchio A; Ackermann L Mangana(III/IV)electro-catalyzed C(sp^3)—H azidation. Chem. Sci 2021, 12 (8), 2890–2897.

(30). Huang X; Bergsten TM; Groves JT Manganese-Catalyzed Late-Stage Aliphatic C—H Azidation. J. Am. Chem. Soc 2015, 137 (16), 5300–5303. [PubMed: 25871027]

(31). Suh S-E; Chen S-J; Mandal M; Guzei IA; Cramer CJ; Stahl SS Site-Selective Copper-Catalyzed Azidation of Benzylic C—H Bonds. J. Am. Chem. Soc 2020, 142 (26), 11388–11393. [PubMed: 32539355]

(32). Bao X; Wang Q; Zhu J Copper-catalyzed remote C(sp^3)—H azidation and oxidative trifluoromethylation of benzohydrazides. Nat. Commun 2019, 10 (1), 769. [PubMed: 30770833]

(33). Ge L; Zhou H; Chiou M-F; Jiang H; Jian W; Ye C; Li X; Zhu X; Xiong H; Li Y; Song L; Zhang X; Bao H Iron-catalysed asymmetric carboazidation of styrenes. Nat. Catal 2021, 4 (1), 28–35.

(34). Lv D; Sun Q; Zhou H; Ge L; Qu Y; Li T; Ma X; Li Y; Bao H Iron–Catalyzed Radical Asymmetric Aminoazidation and Diazidation of Styrenes. Angew. Chem. Int. Ed 2021, 60 (22), 12455–12460.

(35). Messinis AM; Luckham SLJ; Wells PP; Gianolio D; Gibson EK; O'Brien HM; Sparkes HA; Davis SA; Callison J; Elorriaga D; Hernandez-Fajardo O; Bedford RB The highly surprising behaviour of diphosphine ligands in iron-catalysed Negishi cross-coupling. Nat. Catal 2019, 2 (2), 123–133.

(36). Furstner A Iron Catalysis in Organic Synthesis: A Critical Assessment of What It Takes To Make This Base Metal a Multitasking Champion. ACS Cent. Sci 2016, 2 (11), 778–789. [PubMed: 27981231]

(37). Bedford RB How Low Does Iron Go? Chasing the Active Species in Fe-Catalyzed Cross-Coupling Reactions. Acc. Chem. Res 2015, 48 (5), 1485–1493. [PubMed: 25916260]

(38). Yan M; Lo JC; Edwards JT; Baran PS Radicals: Reactive Intermediates with Translational Potential. J. Am. Chem. Soc 2016, 138 (39), 12692–12714. [PubMed: 27631602]

(39). Fischer H The Persistent Radical Effect: A Principle for Selective Radical Reactions and Living Radical Polymerizations. Chem. Rev 2001, 101 (12), 3581–3610. [PubMed: 11740916]

(40). Qiu Y; Hartwig JF Mechanism of Ni-Catalyzed Oxidations of Unactivated C(sp^3)—H Bonds. J. Am. Chem. Soc 2020, 142 (45), 19239–19248. [PubMed: 33111517]

(41). Li G-X; Morales-Rivera CA; Wang Y; Gao F; He G; Liu P; Chen G Photoredox-mediated Minisci C—H alkylation of N-heteroarenes using boronic acids and hypervalent iodine. Chem. Sci 2016, 7 (10), 6407–6412. [PubMed: 28451096]

(42). Li G-X; Morales-Rivera CA; Gao F; Wang Y; He G; Liu P; Chen G A unified photoredox-catalysis strategy for C(sp^3)—H hydroxylation and amidation using hypervalent iodine. Chem. Sci 2017, 8 (10), 7180–7185. [PubMed: 29081950]

(43). Lo JC; Kim D; Pan C-M; Edwards JT; Yabe Y; Gui J; Qin T; Gutiérrez S; Giacoboni J; Smith MW; Holland PL; Baran PS Fe-Catalyzed C—C Bond Construction from Olefins via Radicals. J. Am. Chem. Soc 2017, 139 (6), 2484–2503. [PubMed: 28094980]

(44). Kim D; Rahaman SMW; Mercado BQ; Poli R; Holland PL Roles of Iron Complexes in Catalytic Radical Alkene Cross-Coupling: A Computational and Mechanistic Study. J. Am. Chem. Soc 2019, 141 (18), 7473–7485. [PubMed: 31025567]

(45). Nam W; Lee Y-M; Fukuzumi S Hydrogen Atom Transfer Reactions of Mononuclear Nonheme Metal–Oxygen Intermediates. Acc. Chem. Res 2018, 51 (9), 2014–2022. [PubMed: 30179459]

(46). Huang L; Xun X; Zhao M; Xue J; Li G; Hong L Copper-Catalyzed Regioselective sp^3 C—H Azidation of Alkyl Substituents of Indoles and Tetrahydrocarbazoles. J. Org. Chem 2019, 84 (18), 11885–11890. [PubMed: 31469287]

(47). Nomura K; Sidokmai W; Imanishi Y Ethylene Polymerization Catalyzed by Ruthenium and Iron Complexes Containing 2,6-Bis(2-oxazolin-2-yl)pyridine (Pybox) Ligand-Cocatalyst System. Bull. Chem. Soc. Jpn 2000, 73 (3), 599–605.

(48). Chen T; Yang L; Gong D; Huang K-W Synthesis, crystal structure and reactivity studies of iron complexes with pybox ligands. Inorg. Chim. Acta 2014, 423, 320–325.

(49). Dutta SK; Werner R; Flörke U; Mohanta S; Nanda KK; Haase W; Nag K Model Compounds for Iron Proteins. Structures and Magnetic, Spectroscopic, and Redox Properties of $Fe^{III}M^{II}$ and $[Co^{III}Fe^{III}]_2O$ Complexes with (μ-Carboxylato)bis(μ-phenoxo)-dimetalate and (μ-Oxo)diiron(III) Cores. Inorg. Chem 1996, 35 (8), 2292–2300. [PubMed: 11666427]

(50). Grapperhaus CA; Mienert B; Bill E; Weyhermüller T; Wieghardt K Mononuclear (Nitrido)iron(V) and (Oxo)iron(IV) Complexes via Photolysis of $[(cyclam\text{-}acetato)Fe^{III}(N_3)]^+$

and Ozonolysis of [(cyclam-acetato)$Fe^{III}(O_3SCF_3)]^+$ in Water/Acetone Mixtures. Inorg. Chem 2000, 39 (23), 5306–5317. [PubMed: 11187471]

(51). Meyer K; Bill E; Mienert B; Weyhermuller T; Wieghardt K Photolysis of *cis*- and *trans*-$[Fe^{III}(cyclam)(N_3)_2]^+$ Complexes: Spectroscopic Characterization of a Nitridoiron(V) Species. J. Am. Chem. Soc 1999, 121 (20), 4859–4876.

(52). In this experiment ca. 0.73 equiv of the ^{i}PrPybox ligand was liberated, indicating that ^{i}PrPybox was a weakly coordinated ancillary ligand.

(53). Sabenya G; Lázaro L; Gamba I; Martin-Diaconescu V; Andris E; Weyhermüller T; Neese F; Roithova J; Bill E; Lloret-Fillol J; Costas M Generation, Spectroscopic, and Chemical Characterization of an Octahedral Iron(V)-Nitrido Species with a Neutral Ligand Platform. J. Am. Chem. Soc 2017, 139 (27), 9168–9177. [PubMed: 28598599]

(54). See the Supporting Information for more details.

(55). To ascertain whether the putative iron(III)-azide complex could transfer an azide moiety to an alkyl radical, Fe-3 was generated in situ and heated at 80 °C with AIBN in acetonitrile for 24 h. This reaction formed the alkyl azide. This observation is consistent with reaction of an alkyl radical with the iron(III)-azide species to form the alkyl azide product and the starting iron(II) complex.

(56). Charpentier J; Früh N; Togni A Electrophilic Trifluor-omethylation by Use of Hypervalent Iodine Reagents. Chem. Rev 2015, 115 (2), 650–682. [PubMed: 25152082]

(57). Yasu Y; Koike T; Akita M Three-component Oxytrifluoromethylation of Alkenes: Highly Efficient and Regioselective Difunctionalization of C-C Bonds Mediated by Photoredox Catalysts. Angew. Chem., Int. Ed 2012, 51 (38), 9567–9571.

(58). Attempts to synthesize and isolate (**L1**)$FeCl_2$(2-I-benzoate) were performed but the outcome was inconclusive. See the Supporting Information for further information.

(59). Fawcett A; Keller MJ; Herrera Z; Hartwig JF Site Selective Chlorination of C(sp^3)-H Bonds Suitable for Late-Stage Functionalization. Angew. Chem., Int. Ed 2021, 60 (15), 8276–8283.

(60). (**L1**)$Fe(OAc)_2$(*o*-I-benzoate) could be generated in situ by reaction of **Fe-2** with dimer **4**. See the Supporting Information for more details.

(61). Wang Y; Li G-X; Yang G; He G; Chen G A visible-light-promoted radical reaction system for azidation and halogenation of tertiary aliphatic C—H bonds. Chem. Sci 2016, 7 (4), 2679–2683. [PubMed: 28660040]

(62). **1** and TEMPO were allowed to react in acetonitrile at 50 °C, and the mixture was analyzed by HRMS to determine TEMPO-iodanyl adduct had formed, suggesting λ^2-iodanyl radicals are formed under these conditions. We were unable to detect TEMPO-N3.

(63). Yang J-D; Li M; Xue X-S Computational I(III)-X BDEs for Benziodoxol(on)e-based Hypervalent Iodine Reagents: Implications for Their Functional Group Transfer Abilities. Chin. J. Chem 2019, 37 (4), 359–363.

(64). Wang Y; Hu X; Morales-Rivera CA; Li G-X; Huang X; He G; Liu P; Chen G Epimerization of Tertiary Carbon Centers via Reversible Radical Cleavage of Unactivated C(sp^3)—H Bonds. J. Am. Chem. Soc 2018, 140 (30), 9678–9684. [PubMed: 29983059]

(65). Li G-X; Hu X; He G; Chen G Photoredox-Mediated Minisci-type Alkylation of N-Heteroarenes with Alkanes with High Methylene Selectivity. ACS Catal 2018, 8 (12), 11847–11853.

(66). Yuan Y-A; Lu D-F; Chen Y-R; Xu H Iron-Catalyzed Direct Diazidation for a Broad Range of Olefins. Angew. Chem., Int. Ed 2016, 55 (2), 534–538.

(67). Tingoli M; Tiecco M; Chianelli D; Balducci R; Temperini A Novel azido-phenylselenenylation of double bonds. Evidence for a free-radical process. J. Org. Chem 1991, 56 (24), 6809–6813.

(68). Zhang B; Studer A Stereoselective Radical Azidooxygenation of Alkenes. Org. Lett 2013, 15 (17), 4548–4551. [PubMed: 23930944]

(69). Kösel T; Schulz G; Dräger G; Kirschning A Photochemical Transformations with Iodine Azide after Release from an Ion-Exchange Resin. Angew. Chem., Int. Ed 2020, 59 (30), 12376–12380.

(70). Ward GA; Wright CM Investigation of the anodic oxidation of azide ion on platinum electrodes. J. Electroanal. Chem 1964, 8 (4), 302–309.

(71). It should be noted that substituents *ortho* to iodine can influence hypervalent twisting and may lead to non-representitive reactivity; see the following for more information: Su JT; Goddard WA

Enhancing 2-Iodoxybenzoic Acid Reactivity by Exploiting a Hypervalent Twist. J. Am. Chem. Soc 2005, 127 (41), 14146–14147. [PubMed: 16218584]

(72). Added dimer 4 inhibited the azidation reaction, but the origins of this effect were unclear. See the Supporting Information for more information.

(73). Beckwith ALJ; Moad G The kinetics and mechanism of ring opening of radicals containing the cyclobutylcarbinyl system. J. Chem. Soc., Perkin Trans. 2 1980, 2 (7), 1083.

(74). Emanuel CJ; Horner JH; Newcomb M Rate constants for ring openings of 2-phenylcyclobutyl-carbinyl radicals. J. Phys. Org. Chem 2000, 13, 688–692.

(75). Lonca GH; Ong DY; Tran TMH; Tejo C; Chiba S; Gagosz F Anti-Markovnikov Hydrofunctionalization of Alkenes: Use of a Benzyl Group as a Traceless Redox-Active Hydrogen Donor. Angew. Chem., Int. Ed 2017, 56 (38), 11440–11444.

(76). Wang JJ; Yu W Anti-Markovnikov Hydroazidation of Alkenes by Visible-Light Photoredox Catalysis. Chem. - Eur. J 2019, 25 (14), 3510–3514. [PubMed: 30648294]

(77). We assume an equilibrium between the combination of an iron-carboxylate and HN_3 and the combination of iron-azide and carboxylic acid could be occurring.

(78). Luo Y-R Comprehensive Handbook of Chemical Bond Energies; CRC Press, 2007.

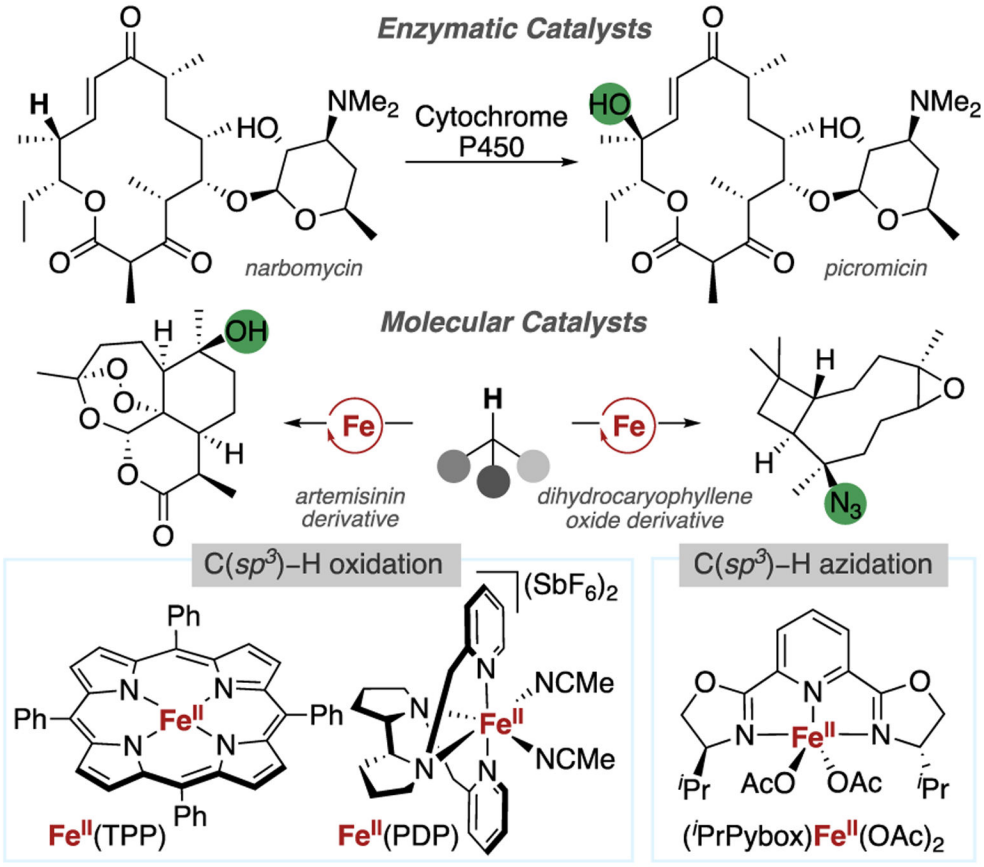

Figure 1.
Iron catalysts and their applications in complex molecule functionalization.

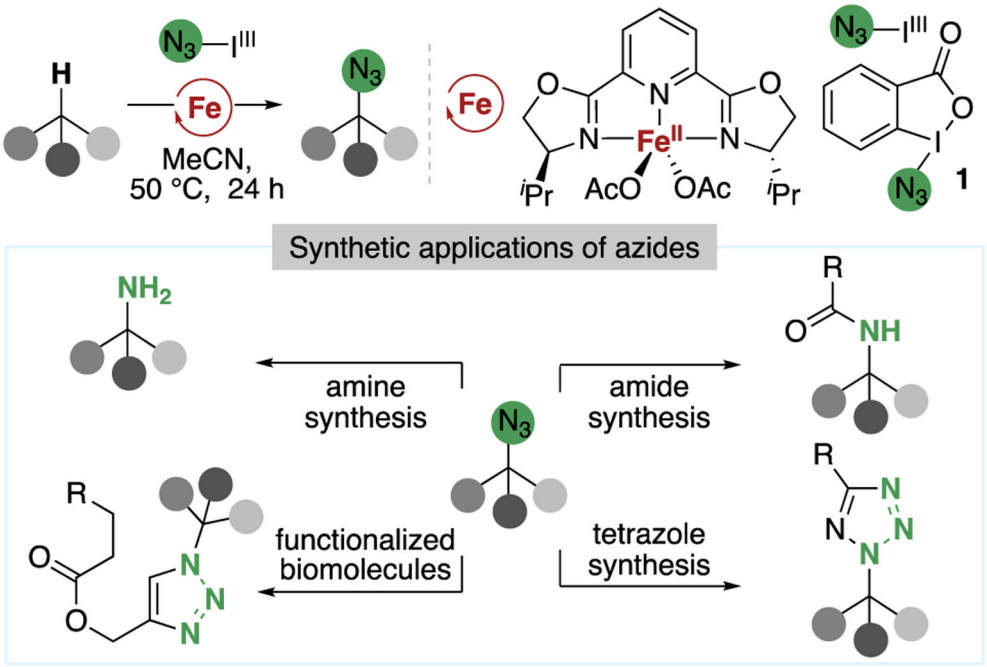

Figure 2.
Iron-catalyzed C(sp^3)—H azidation and the synthetic applications of aliphatic azides.

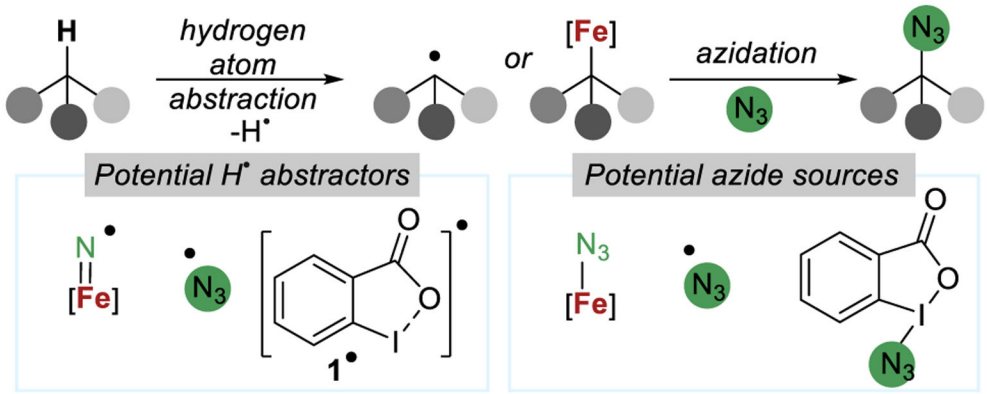

Figure 3.

Plausible species involved in the mechanism of the iron-catalyzed azidation of C(sp^3)—H bonds with Zhdankin's λ^3-azidoiodane.

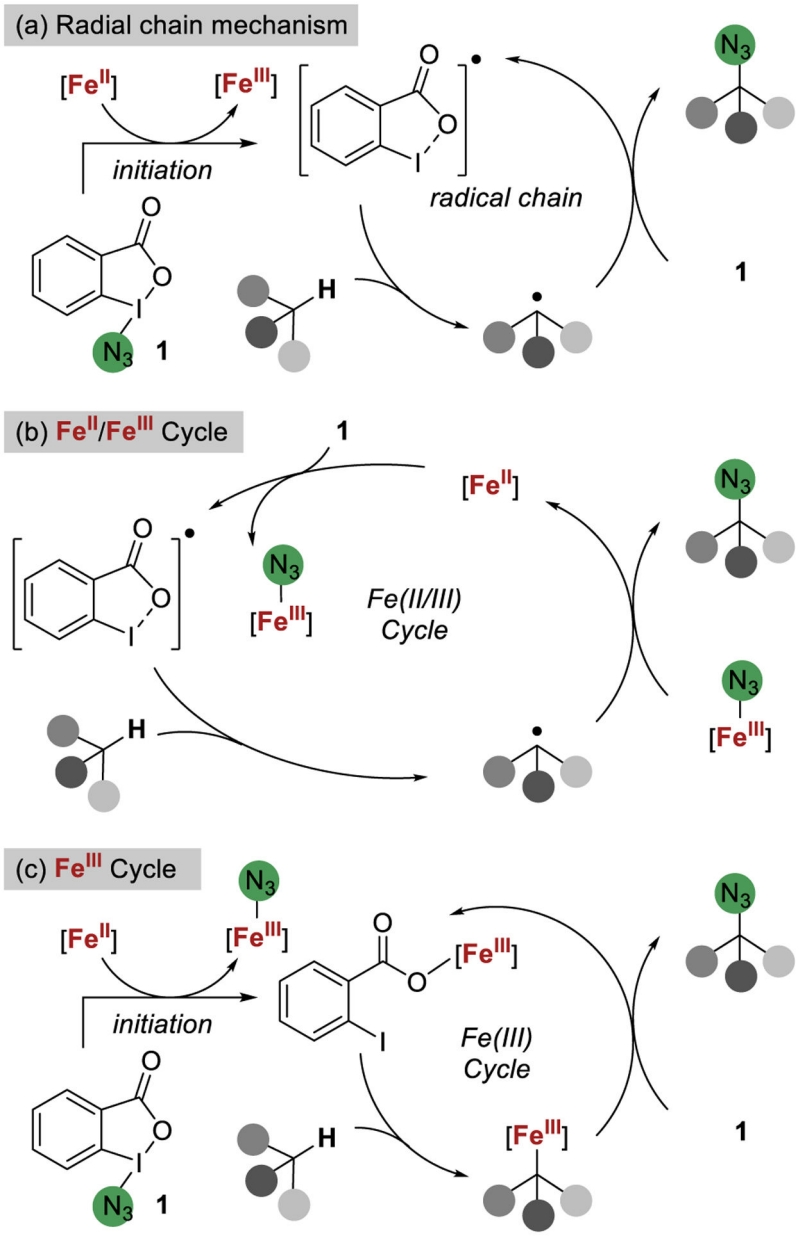

Figure 4.

Distinct catalytic cycles proposed. (a) Radical chain mechanistic proposal. (b) Iron-azide radical mechanism. (c) Iron-catalyzed C—H cleavage mechanism.

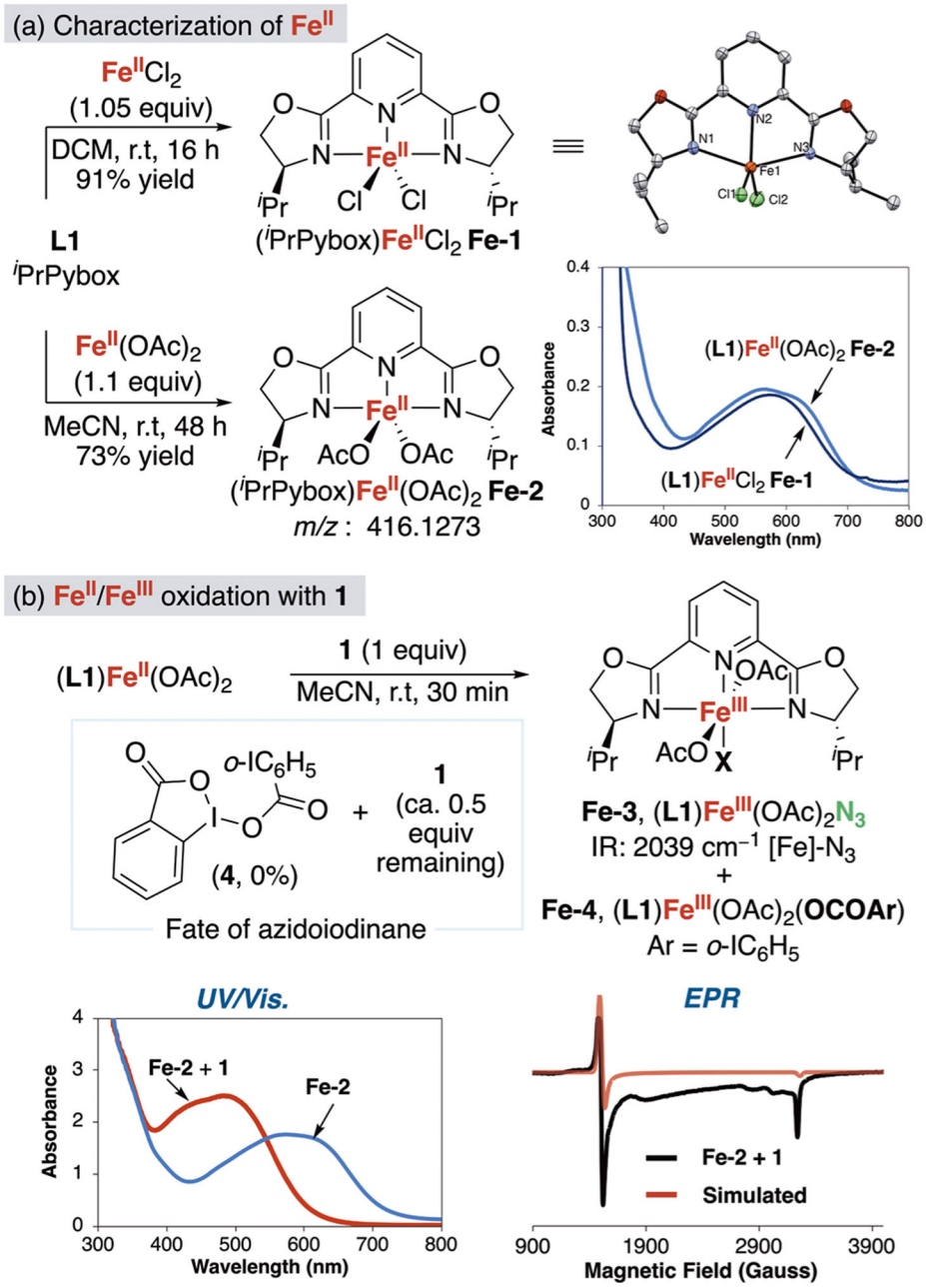

Figure 5.

(a) Preparation, isolation, and characterization of (^{i}PrPybox)FeCl$_2$ (**Fe-1**) and (^{i}PrPybox)Fe(OAc)$_2$ (**Fe-2**). (b) Reaction of **Fe-2** with λ^3-azidoiodane **1** and analysis of the iron-containing reaction products by ATR-IR, UV/vis absorption, and EPR spectroscopy.

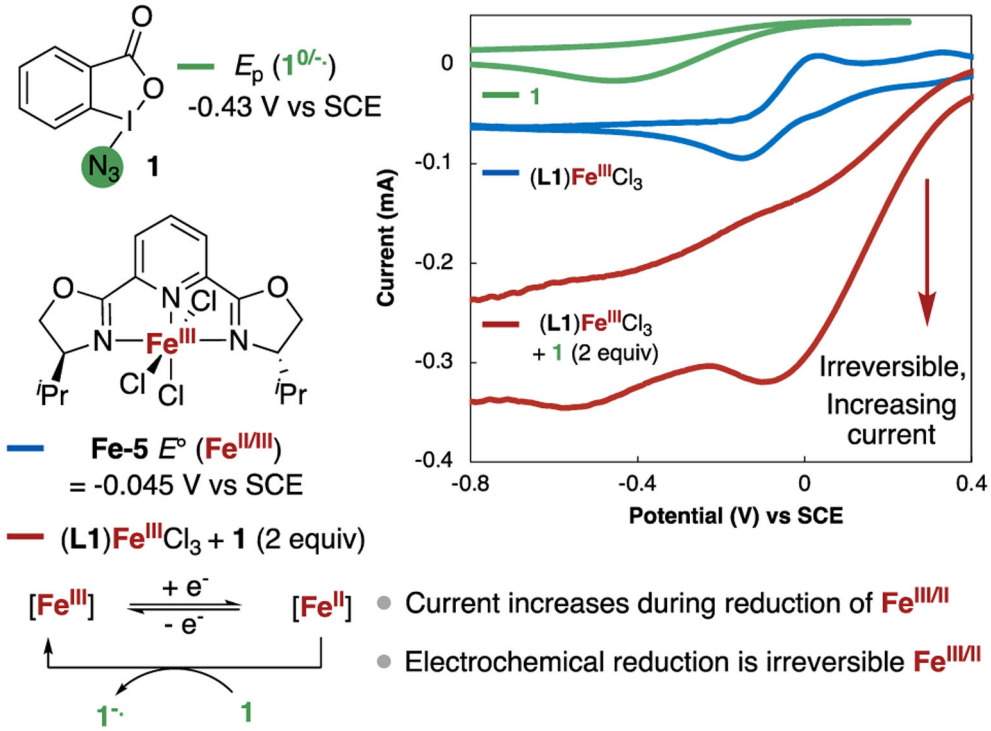

Figure 6.

Cyclic voltammetry of Fe-5 and **1**, and investigating the chemical oxidation of Fe(II) to Fe(III) by **1** in MeCN containing 0.1 M [$^{n}Bu_4N$][PF_6] as electrolyte with a glassy carbon working electrode at a scan rate of 200 mV/s.

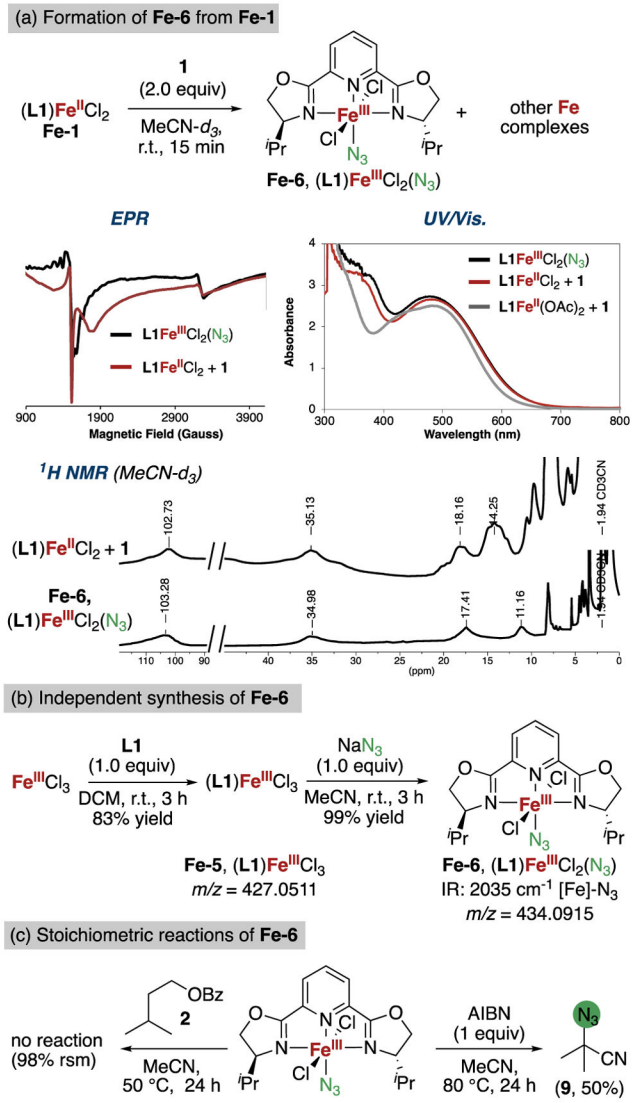

Figure 7.

(a) Formation of **Fe-6** by the oxidation of **Fe-1** with **1** and analysis of the reaction mixture by EPR, UV/vis, and ^{1}H NMR spectroscopy. (b) Preparation of (**L1**)$FeCl_2(N^3)$ (**Fe-6**). (c) Stoichiometric reactions of **Fe-6**.

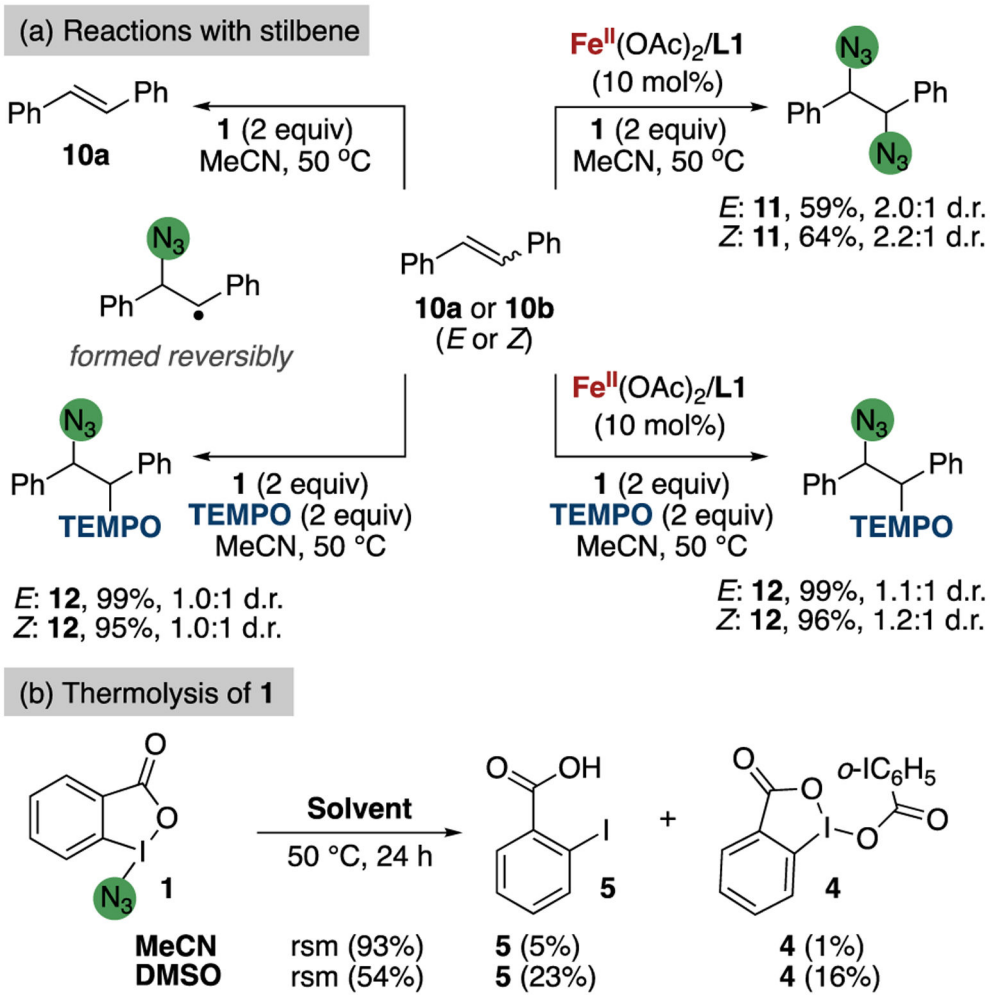

Figure 8.

Homolysis of **1** and reactions with stilbenes. (a) Reaction of stilbenes under typical C(sp^3)—H bond azidation conditions with and without iron, and conditions with and without iron in the presence of TEMPO. (b) Thermolysis of **1** in DMSO and MeCN.

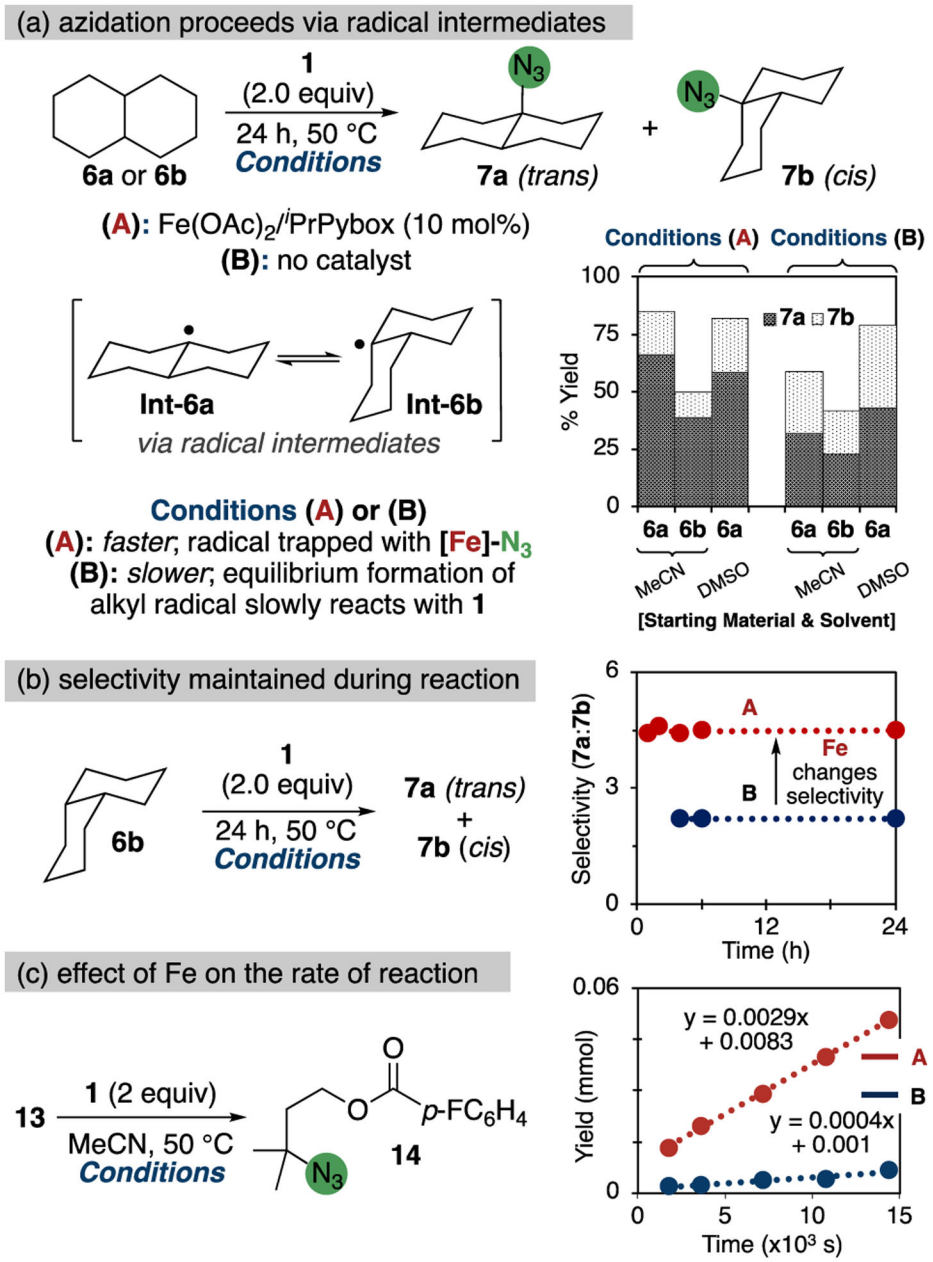

Figure 9.

Summary of results obtained from the azidation of *cis*- and *trans*-decalin. (a) The azidation of *cis*-decalin and *trans*-decalin under a variety of conditions. (b) Monitoring the *trans:cis* ratio of the tertiary azide products in the azidation of cis-decalin throughout the course of the reaction. (c) Monitoring azidation of isopentyl 4-fluorobenzoate under standard catalytic conditions with and without iron.

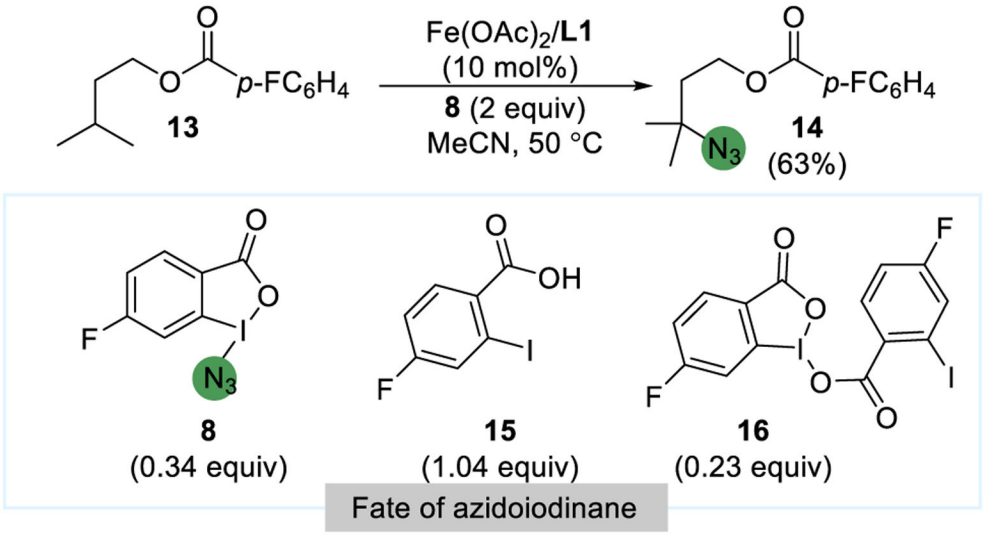

Figure 10.

Investigation of the fate of a fluorinated λ^3-azidoiodane reagent **8** in the azidation of **13**.

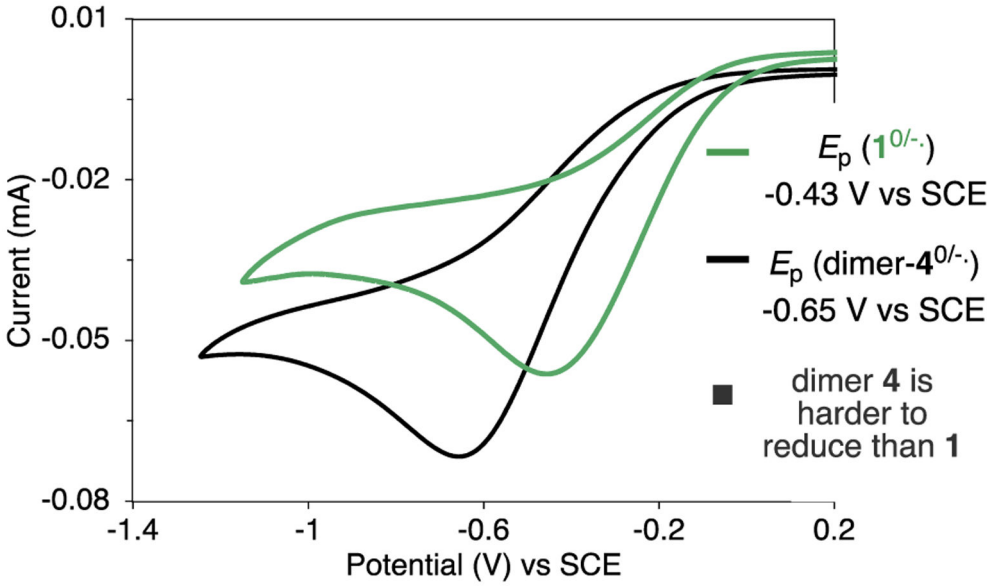

Figure 11.

Cyclic voltammograms of **1** and **4** in MeCN containing 0.1 M [$^{n}Bu_4N$][PF_6] as electrolyte with a glassy carbon working electrode at a scan rate of 200 mV/s.

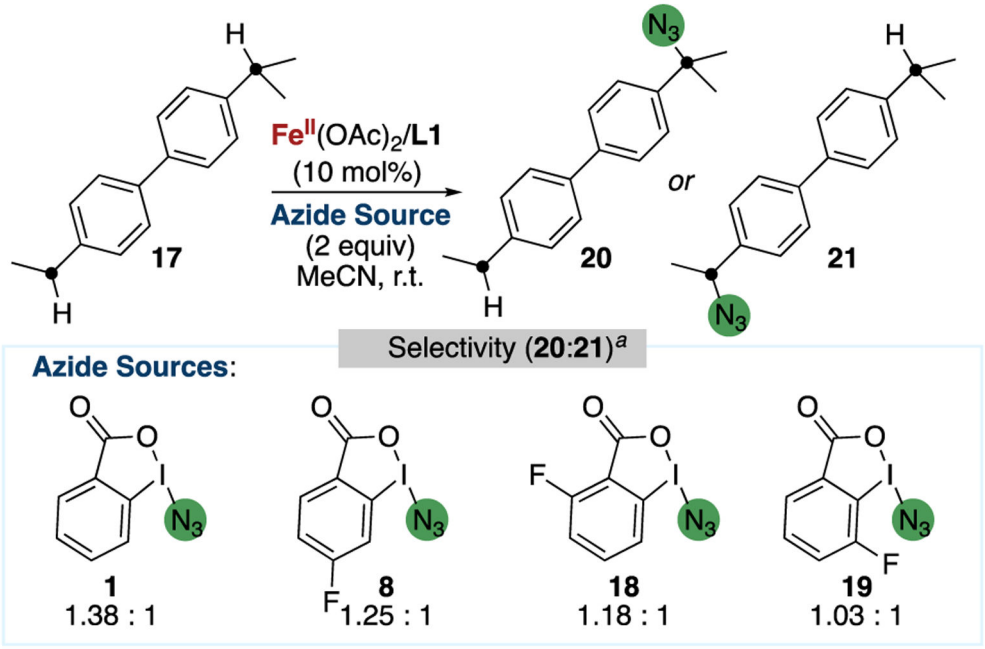

Figure 12.

Effect of substituents on the λ^3-azidoiodane reagent on the regioselectivity of the azidation of secondary and tertiary benzylic C(sp^3)—H bonds of a biphenyl substrate. [a]Error in ratios, ±0.01.

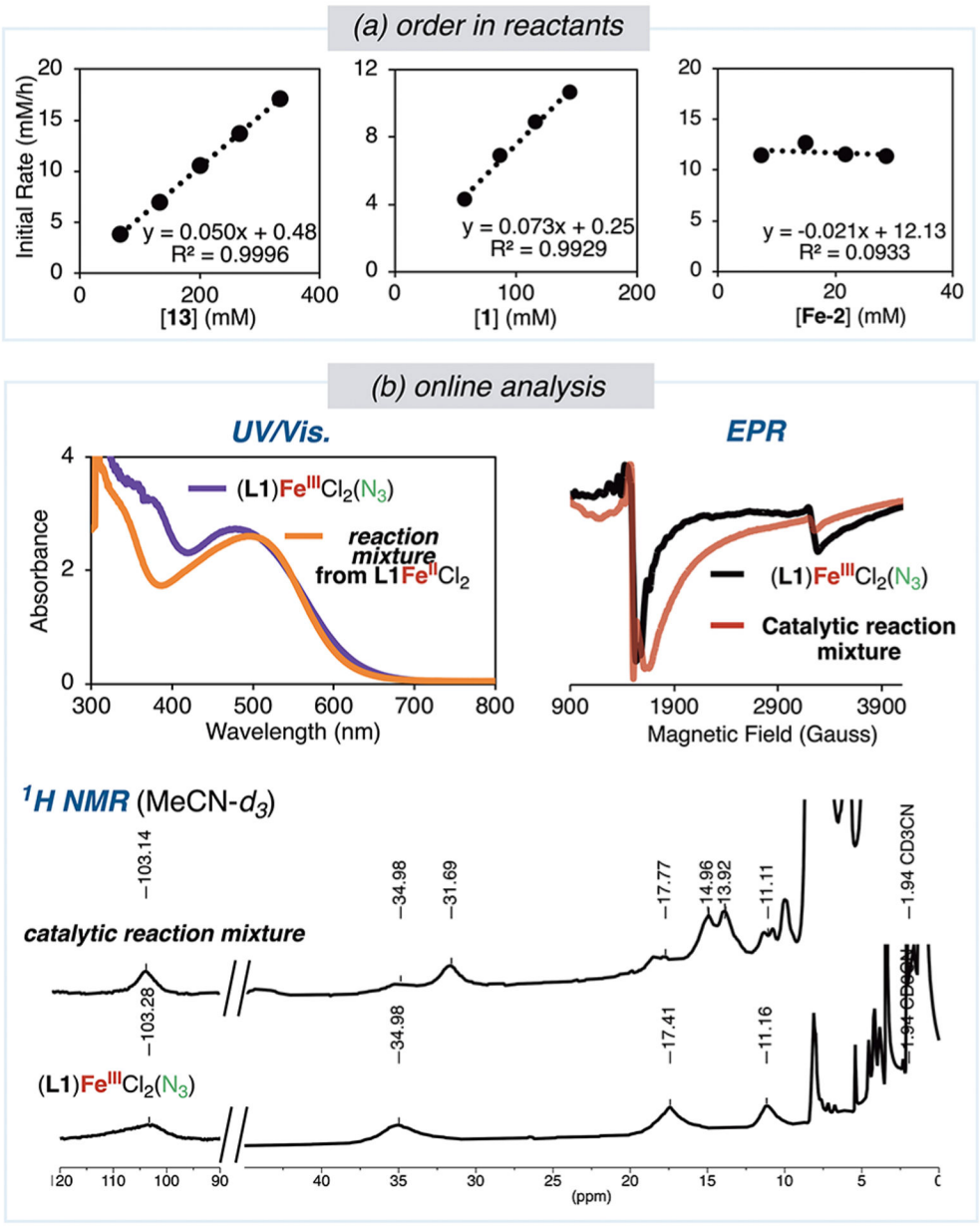

Figure 13.

Kinetic measurements and spectroscopic analysis of the catalytic reaction. (a) Order in reactants determined by measuring initial rates of reaction of **1** with alkyl benzoates **2** or **13** by GC or ^{19}F NMR spectroscopy in MeCN with $Fe(OAc)_2$ and **L1** or **L2** as catalyst. Left: reaction of **1** with **13** in acetonitrile with 0.267 M **1** and 10 mol% $Fe(OAc)_2$ and **L2**; center: reaction of **1** with **2** in acetonitrile with 0.146 M 2 and 10 mol% $Fe(OAc)_2$ and **L1**; right: reaction of **1** with **2** in acetonitrile with 0.291 M **1** and 0.146 M **2** and **L1**. (b) Characterization of the catalytic reaction of **1** with 2 catalyzed by 10 mol% **Fe-1** by UV/vis, EPR, and ^{1}H NMR spectroscopy at 30 min. X-band EPR spectra obtained at 10 K in a 1:1 THF/MeCN solvent mixture.

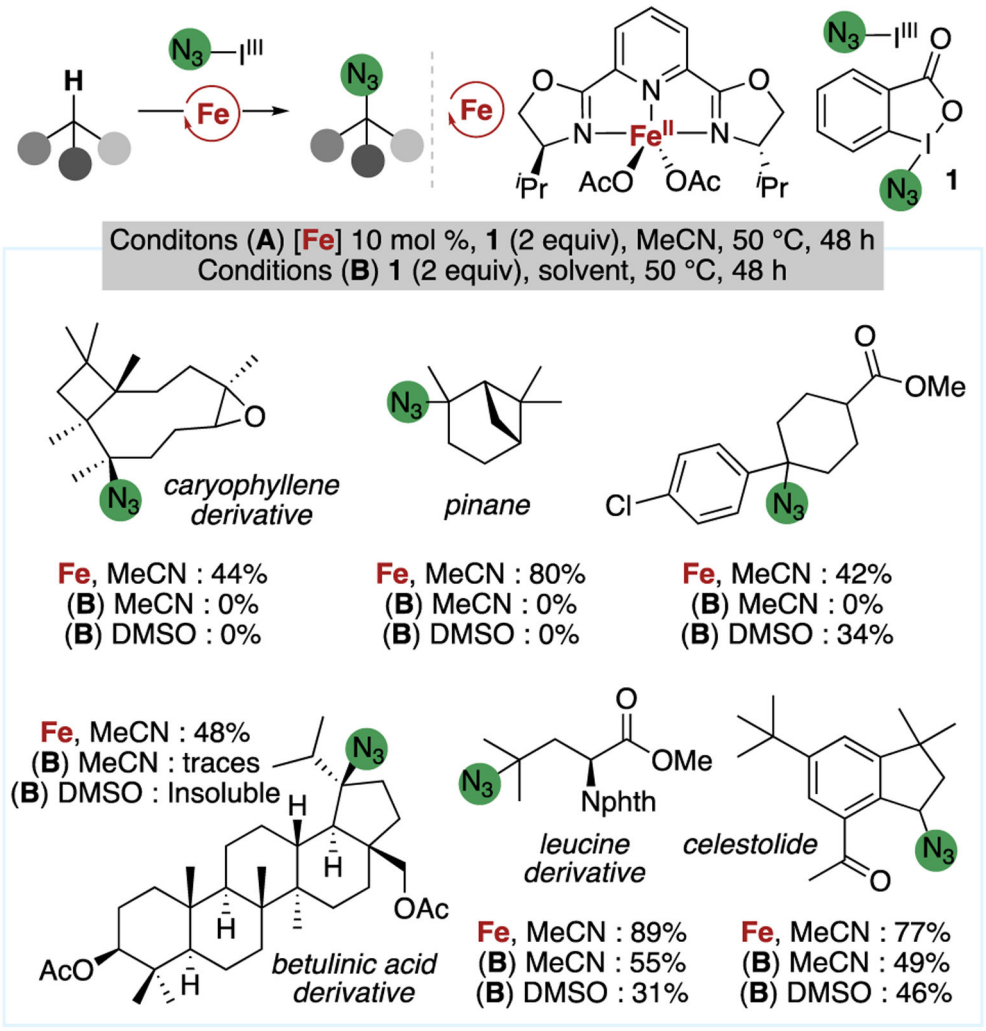

Figure 14.

Summary of results obtained from the azidation of pinane, a derivative of caryophyllene, and several other substrates, under a variety of azidation conditions.

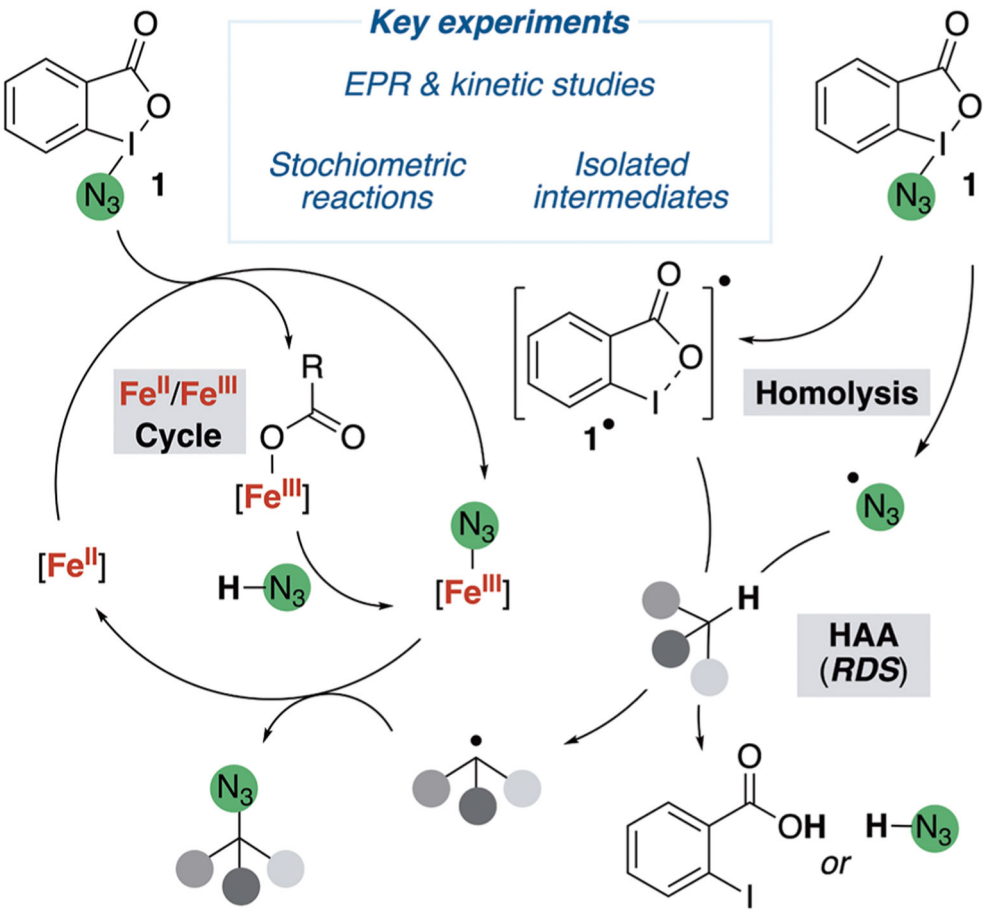

Figure 15.
Proposal for the mechanism of the iron-catalyzed C(sp^3)—H azidation that fits all of the experimental data.